NASA NO. NGR-10-008028

ELASTIC PLATE SPALLATION
FINAL REPORT

by

Larry Oline, Project Director
John Medaglia, Graduate Research Assi

College of Engineering

University of South Florida
Tampa Florida 33620

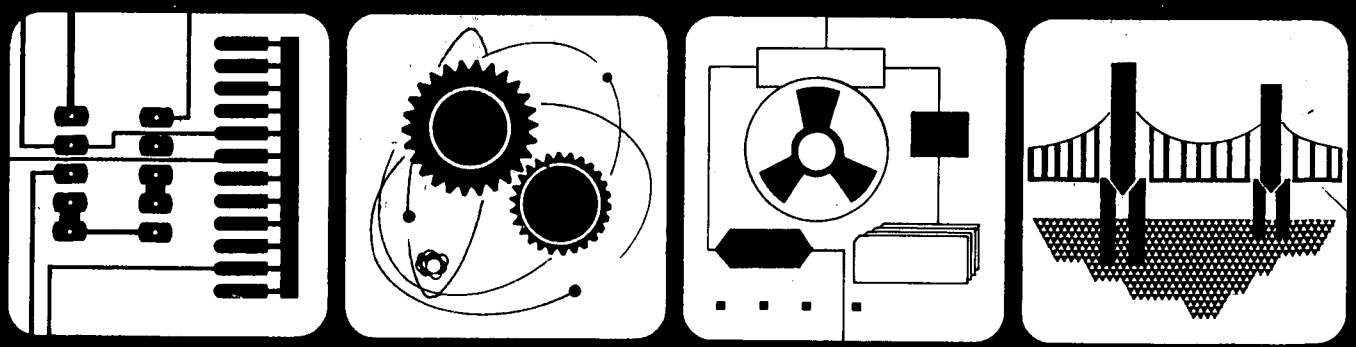

Final Report
Elastic Plate Spallation
Grant: NASA No. NGR-10-008028

Date: May 31, 1972

Larry Oline, Project Director

John Medaglia, Graduate Research Assistant

TABLE OF CONTENTS

LIST OF TABLES

LIST OF FIGURES

LIST OF SYMBOLS

A	Area
B	Matrix relating strain and displacement
D	Matrix relating stress and strain by Hooke's Law
DE	Element size
E	Young's modulus of elasticity
H	Plate thickness
KELM	Element stiffness matrix
KASY	Assembled stiffness matrix
R	Radial coordinate
R_i	Externally applied force to a node
S_i	Nodal force
U_i	Laplace transform of displacement
UR	Displacement in radial direction
UZ	Displacement in axial direction
W	Work
Z	Axial coordinate
α_i	Constants in displacement functions (i = 1,...,6)
γ	Shear strain
δ	Matrix of all nodal displacements
δ_e	Matrix of element nodal displacements
δ_i	Nodal displacement
ε	Strain

λ	Lamé constant = $\frac{\nu E}{(1 + \nu)(1 - 2\nu)}$
μ	Lamé constant = $\frac{E}{2(1 + \nu)}$ = shear modulus
ν	Poisson's ratio
π	Constant = 3.14159
σ	Stress
τ	Shear stress

CHAPTER I

INTRODUCTION

Spallation is a failure condition caused by stress wave interaction from blast or impact loading of an object. The most common example is the conical hole produced in glass by the impact of a pellet. In more ductile materials, such as aluminum, a spall may be as subtle as the formation of an internal void or as dramatic as in glass, with the casting off of a chunk from the side of the plate opposite to the side impacted.

Previous work on stress waves and spallation has been done analytically, experimentally, and numerically. There is a great deal of work on infinite half-spaces, but only a few studies on plates, which are applicable and necessary in order to understand spallation of plates. Davids [1][1] has solved the problem of waves generated by a point load applied to a plate both before and after reflecting from the back face. A recent paper by Viswanathan and Biswas [2] studies waves in a plate produced by distributed loads. Their work is also analytical. Dally and Riley [3] have used dynamic photoelasticity to study stress waves in

---

[1]Numbers in brackets, [], refer to the Bibliography.

a plate, but their work is not general. Ang and Newmark [4] studied stress waves by a finite difference technique but did not discuss reflections or spallation. Costantino [5] outlined the finite element method for studying stress waves but did not investigate the waves in detail or investigate reflections and spallation.

Figure 1 shows an experimentally produced spall in an aluminum plate. Obviously, large plastic and hydrodynamic forces were present in the total response of the plate to the impact. While a numerical scheme could be developed to approximate the total phenomenon, it is not necessary. The material must pass through the elastic range on the way to a spall condition. Investigation of the elastic waves alone will show which ones interact and where they interact to develop high stresses. These interactions and stresses may be interpreted for their contribution to spallation.

The research presented here uses dynamic finite elements to investigate elastic stress waves in a plate. The investigation will discuss all waves produced by point and distributed loads applied to a plate. Conclusions will be drawn as to their importance in spallation.

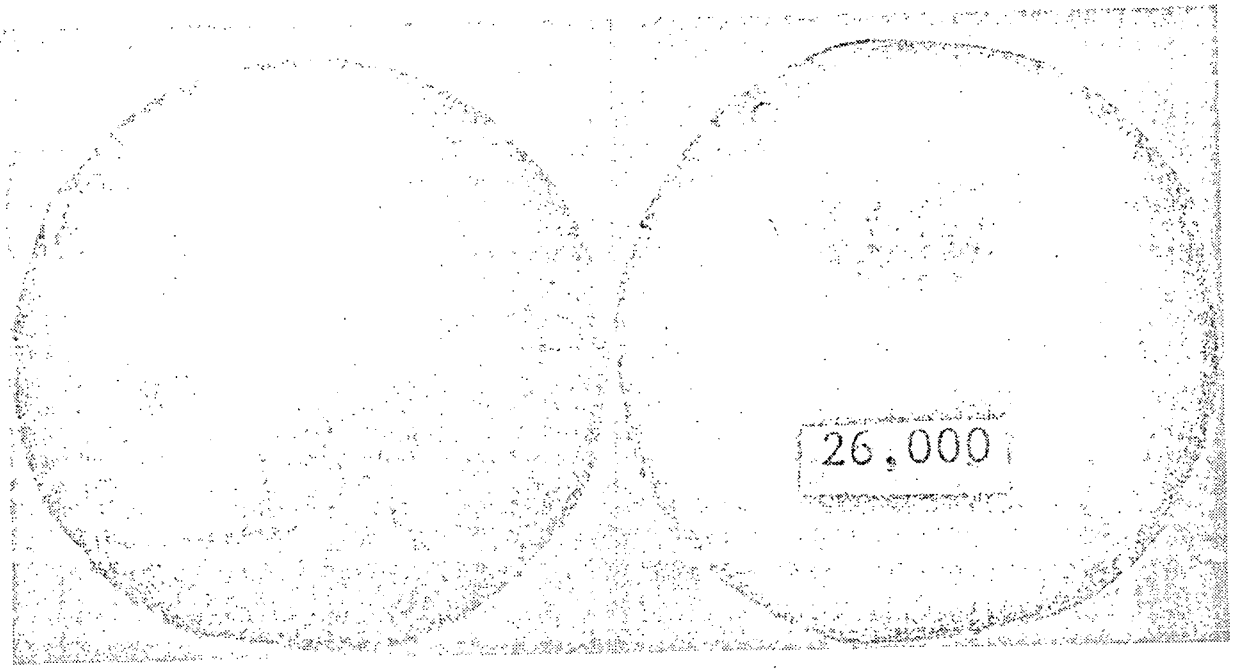

a) Front face

b) Back face

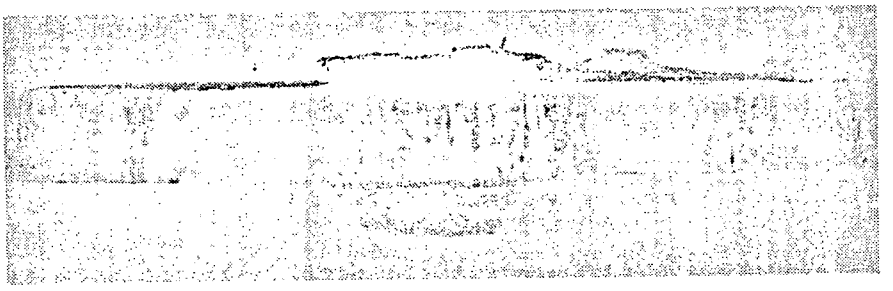

c) Edge view

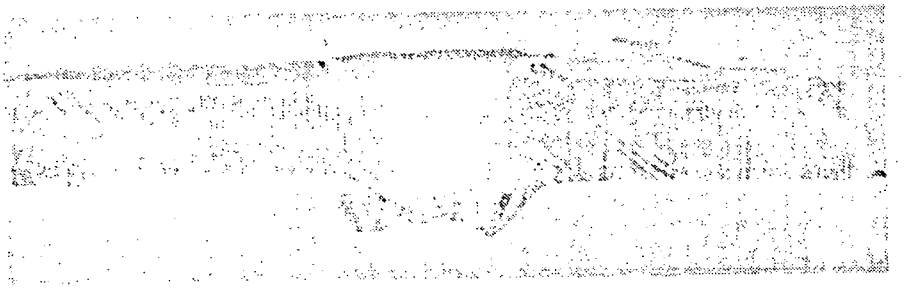

d) Cross section

Figure 1. Experimentally Produced Spall in an Aluminum Plate

CHAPTER II

FINITE ELEMENT METHOD

A short description of the finite element method in general is given first to outline the salient points of the method. Then a more detailed description of the specific method for axisymmetric problems is given. The discussion of the axisymmetric dynamic finite element method also outlines the program used for this research. Detailed derivations of the items mentioned are in Appendix A. The program is listed in Appendix C.

General Method

The general finite element approach to the analysis of any continuous body may be listed in seven steps. These are as follows:

1. Divide the body into suitable pieces or elements;
2. Assume a displacement function for displacements in an element. Compatability is insured because the functions include parameters defined in terms of nodal displacements;

3. Nodes are the intersections of the imaginary lines and planes used to divide the continuum into elements. The geometric locations of the nodes must be recorded and also which nodes correspond to each element;
4. Using force equilibrium at the nodes and virtual work, the elements are combined to a system of equations approximating the body. The equations involve stiffness, displacement, and applied forces;
5. If the problem is dynamic, the inertia must be accounted for in the equations developed in the previous step. For transient wave problems, the mass is lumped at the nodes. Standing wave problems should be solved with the "consistent" mass matrix which is derived by virtual work with the inertia forces treated as distributed body forces. The mass matrix times accelerations of the nodes is added to the static equations of step (4);
6. The system of equations is solved for nodal displacements;
7. Once the nodal displacements are known, they are used to find strains element by element which are in turn used to find stresses throughout the body.

In a static problem, the equations formulated in step (4) consist of stiffness terms times nodal displacements

set equal to forces externally applied to the nodes. The nodal displacements are determined by an elimination technique or by inversion of the stiffness matrix. In a dynamic problem, the mass times acceleration terms create second order, linear differential equations. These may be solved by integration, which may be prohibitively difficult, or by rewriting the acceleration in finite difference notation. The resulting algebraic equations are solved stepwise in time. The displacements, strains and stresses change with each time step.

The lumped mass approach is based on a paper by Costantino [5]. The following axisymmetric application is based mainly on a discussion by Zienkiewicz [6].

Dynamic Finite Element Method for Transient Waves in an Axisymmetric Plate

Element Formulation

A circular, symmetric, distributed load applied to an infinite plate produces an axisymmetric response in the plate. The infinite plate is approximated by an axisymmetric disk of finite radius where the radius is great enough so that reflections from the radial boundary do not interfere with reflections from the back face of the plate until after the time of interest. This axisymmetric model is easily divided into axisymmetric finite elements as shown in Figure 2. The elements are triangular in the R-Z plane for simplicity of formulation and are the same as plane

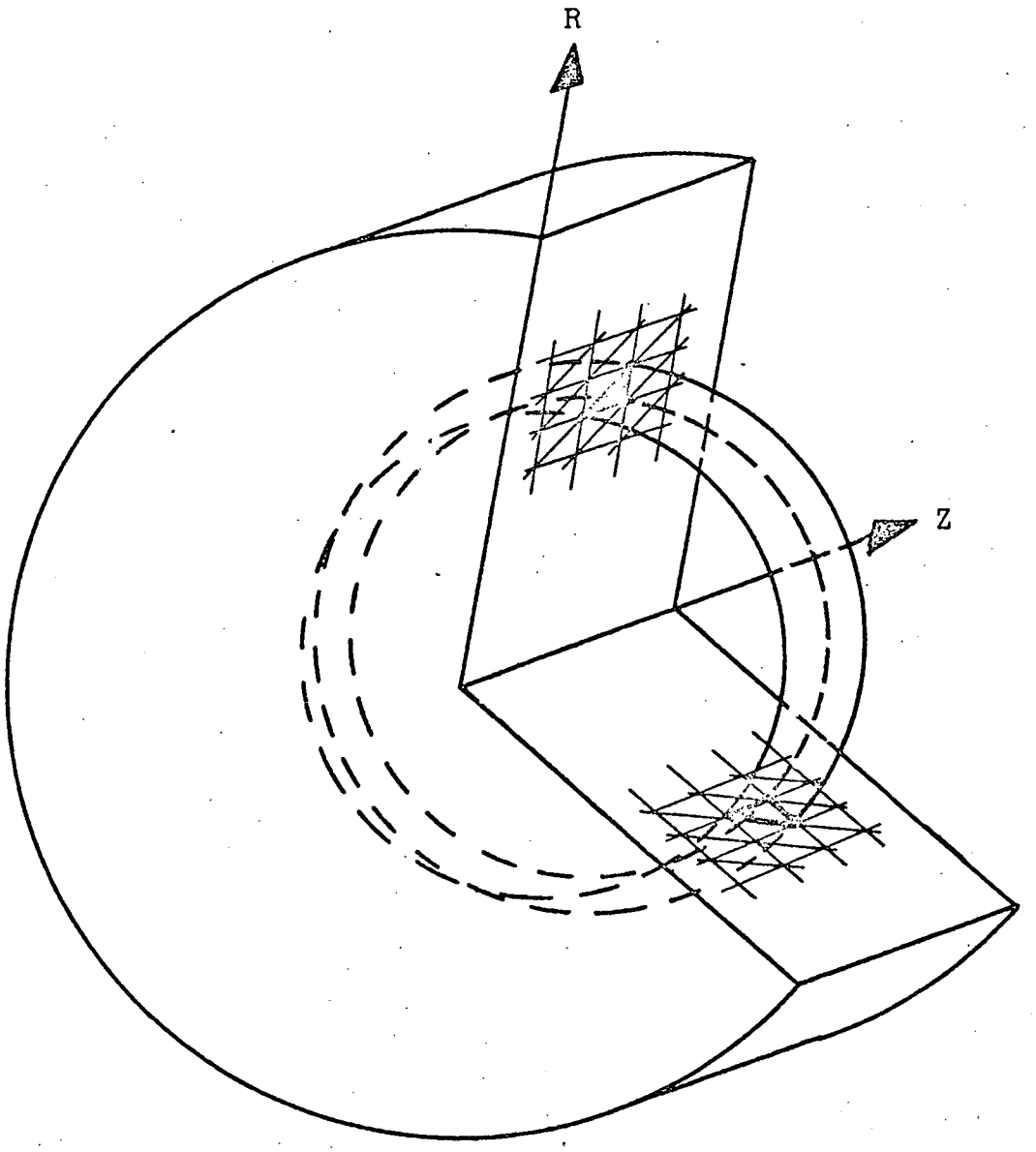

Figure 2. Cutaway of Axisymmetric Finite Elements and Plate

strain elements with the exception that thickness of an element is replaced by centroidal circumference. Also, they must be capable of circumferential strain and stress. Nodal points of plane theory become nodal rings in axisymmetric application. Circumferential effects are a function of radial effects only, so that only radial and axial displacements are required to fully describe the problem. Suitable displacement functions involve one constant for each degree of freedom of the element. This is a Rayliegh-Ritz approximation.

$$UR = \alpha_1 + \alpha_2 R + \alpha_3 Z$$
$$UZ = \alpha_4 + \alpha_5 R + \alpha_6 Z \qquad (1)$$

where α_1 through α_6 are the unknown constants.

R and Z are the coordinate position of the point whose displacement is desired.

UR = radial displacement of the point.

UZ = axial displacement of the point.

The constants, α_i, (i = 1, 2, . . . , 6), may be defined in terms of nodal displacements as is shown in Appendix A. The displacement of any point in an element is then defined by the nodal displacements and the geometric position of the point.

Strain Displacement Relations

From the definition of strain (Fung [7]),

$$\varepsilon_{ij} = \frac{1}{2}(U_{i,\,j} + U_{j,\,i})$$

and the assumption of axial symmetry, only four strains remain.

$$\begin{aligned} \varepsilon_R &= \frac{\partial UR}{\partial R} \\ \varepsilon_\theta &= \frac{UR}{R} \\ \varepsilon_Z &= \frac{\partial UZ}{\partial Z} \\ \gamma_{RZ} &= \frac{\partial UR}{\partial Z} + \frac{\partial UZ}{\partial R} \end{aligned} \tag{2}$$

Equation set (2) can be arranged in matrix form (see Appendix A). These are constant strain elements.

$$\{\varepsilon\}_e = [B]\{\delta\}_e \tag{3}$$

where [B] is a matrix of coefficients based solely on geometry of the element. The matrix $\{\delta\}_e$ is the nodal displacements of the element.

$$\{\delta\}_e = \begin{Bmatrix} UR_i \\ UZ_i \\ UR_j \\ UZ_j \\ UR_m \\ UZ_m \end{Bmatrix}$$

Stress Strain Relation

Hooke's law for axisymmetric problems reduces to four stresses.

$$[D] = \frac{E}{(1+\nu)(1-2\nu)} \begin{bmatrix} (1-\nu) & \nu & \nu & 0 \\ \nu & (1-\nu) & \nu & 0 \\ \nu & \nu & (1-\nu) & 0 \\ 0 & 0 & 0 & \frac{(1-2\nu)}{2} \end{bmatrix}$$

$$\begin{Bmatrix} \sigma_R \\ \sigma_\theta \\ \sigma_Z \\ \tau_{RZ} \end{Bmatrix} = [D] \begin{Bmatrix} \epsilon_R \\ \epsilon_\theta \\ \epsilon_Z \\ \gamma_{RZ} \end{Bmatrix} \tag{4}$$

Stiffness Matrix

Element stiffness may be calculated by the principle of virtual work. The matrix $\{S\}_e$ is the nodal forces resisting deformation of an element. Then from the principle of virtual work:

$$\{S\}_e\{\delta\}_e^T = \int_V \sigma\epsilon dV.$$

Substituting equations (3) and (4) and integrating,

$$\{S\}_e\{\delta\}_e^T = 2\pi \cdot RBAR \cdot A \cdot \{\delta\}_e^T[B]^T[D][B]\{\delta\}_e$$

$$\{S\}_e = 2\pi \cdot RBAR \cdot A \cdot [B]^T[D][B]\{\delta\}_e.$$

RBAR is the radial distance to the centroid of the element. Therefore the stiffness matrix is

$$[K]_e = 2\pi \cdot RBAR \cdot A \cdot [B]^T[D][B]. \tag{5}$$

The stiffness for the system of elements representing the continuous body may be obtained by adding the element stiffnesses in the proper way. This may be done in a tedious fashion by writing force equilibrium at each node of the entire system and also element by element. The terms of the element equilibrium equations are added into the appropriate positions in the set of equations for the entire system. This may be simplified by "globally" numbering the nodes in any orderly sequence and then listing their displacements in a $\{\delta\}$ array for the entire system sequentially from smallest node number to largest. Each element's nodes are called i, j, and m, numbering counterclockwise (See Figure 3). Nodes i, j, and m have values prescribed by the global numbering. Then any number, k_{12}, for example, in the element stiffness matrix adds into a position in the assembled stiffness matrix calculable from the node numbers i, j, or m which correspond to k_{12}.

The element stiffness matrix is 6 x 6 because the element has six degrees of freedom. The order of the assembled stiffness matrix is 2n x 2n where n is the number of nodes and 2 is the number of degrees of freedom per node. However, the assembled stiffness matrix is banded and sparsely populated for the element system of this research. In fact, the maximum number of non-zero terms on any row is fourteen. This is because the greatest number of nodes adjacent to any one node is six; so one node plus six adjacent times two degrees of freedom is fourteen.

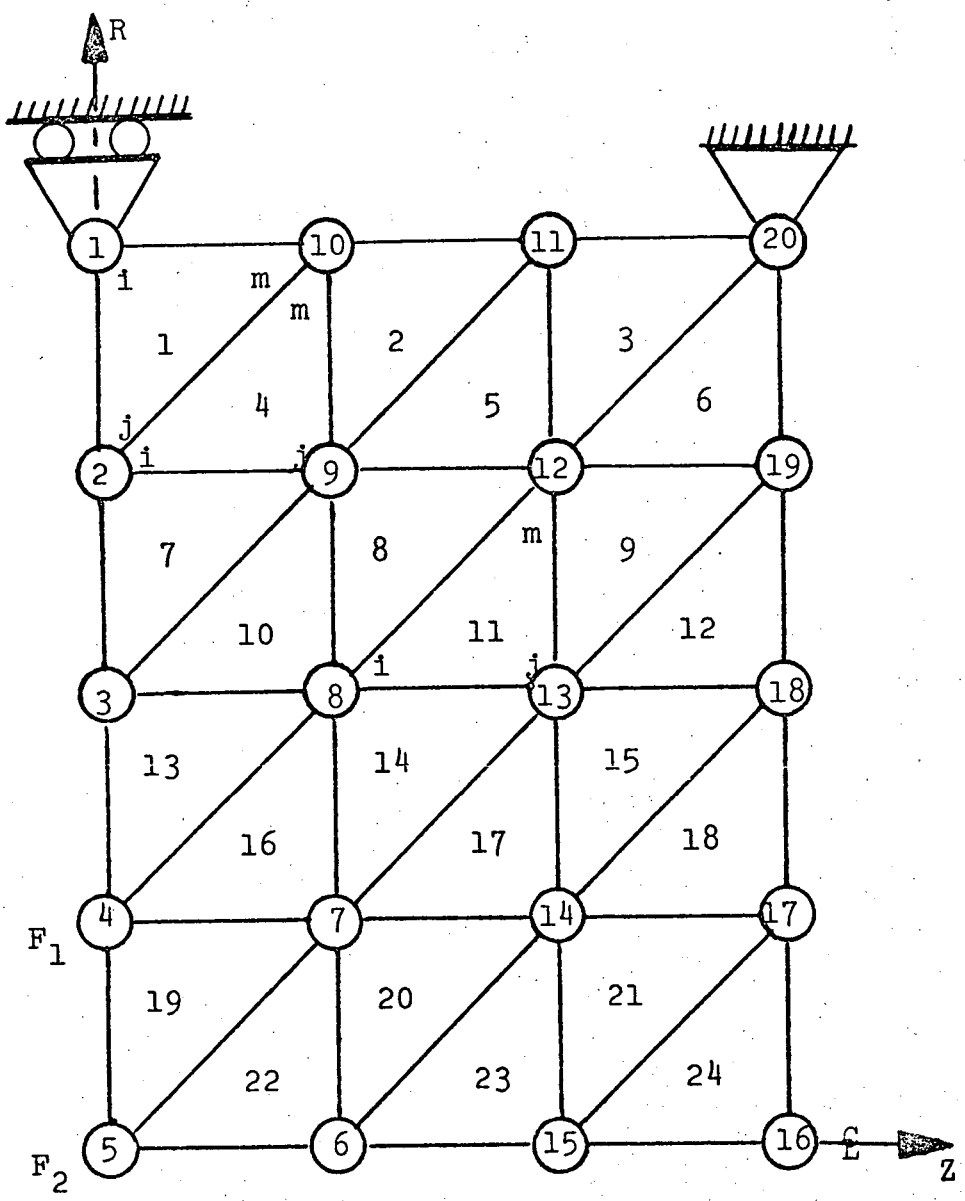

NF	NELM	NNOD	NCL	NFC	NZZ	NZR
2	24	20	2	3	4	8

Figure 3. Typical Node and Element Numbering Scheme

Great savings in core storage are achieved by making use of this fact. An additional matrix called NADJ, composed of the node numbers of each node and the nodes adjacent to it is used to condense the assembled stiffness matrix, KASY, from 2n by 2n to 2n by 14. A further explanation is given in Appendix A.

Mass Matrix

The lumped mass matrix is used in this research because of the assumption made by Costantino [5] that the consistent mass matrix would not allow wave propagation and in fact give rise to an infinite wave speed. That is, all points in the body would feel the disturbance at the same time. Appendix B shows that Costantino's assumption is valid and compares the consistent mass matrix and lumped mass matrix in a simple closed form problem. The consistent mass matrix is derived in Appendix B.

The lumped mass matrix has proven to give appropriate results. The wave speeds are correct and stress distributions follow the correct shape and approximate the correct magnitude as is discussed in Chapter III.

The lumped mass matrix does not require any derivation. The mass of an element is equally divided among its three nodes. A node shared by six elements then has the mass of two elements concentrated at it. A node shared by three elements has the mass of one element and so forth. The lumped mass matrix is diagonal. Formulation of the

mass matrix for this axisymmetric problem is shown in Appendix A.

As an example of the lumped mass matrix consider the mass times acceleration for the following one dimensional bar example.

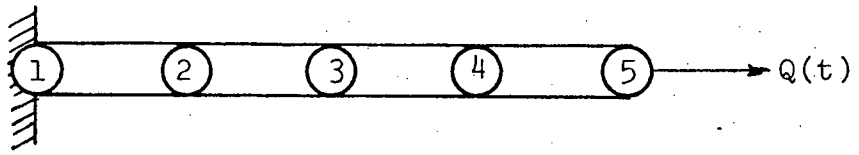

5 nodes, 4 elements

m_0 = mass of one element

$$ma = m_0 \begin{bmatrix} \frac{1}{2} & 0 & 0 & 0 & 0 \\ 0 & 1 & 0 & 0 & 0 \\ 0 & 0 & 1 & 0 & 0 \\ 0 & 0 & 0 & 1 & 0 \\ 0 & 0 & 0 & 0 & \frac{1}{2} \end{bmatrix} \begin{Bmatrix} \ddot{u}_1 \\ \ddot{u}_2 \\ \ddot{u}_3 \\ \ddot{u}_4 \\ \ddot{u}_5 \end{Bmatrix}$$

Equations of Motion

Consider a simple spring and mass system.

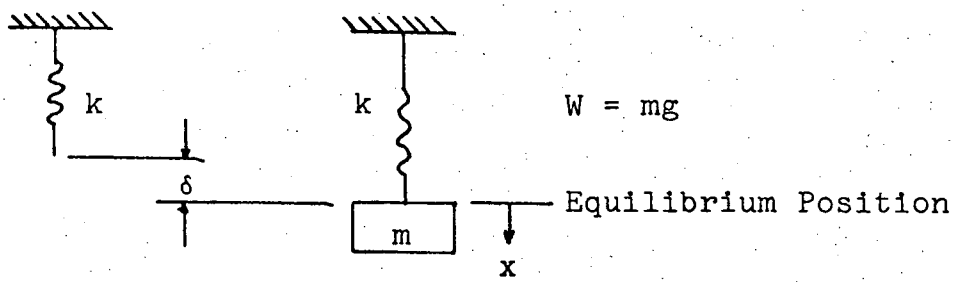

Statically; $\Sigma\bar{F} = 0$

$$-k\delta + W = 0$$

$$k\delta = W$$

Dynamically;

$$\Sigma\bar{F} = m\bar{a}$$

$$-kx + W = m\ddot{x}$$

$$m\ddot{x} + kx = W$$

This approach holds for a complicated system of masses and springs which is exactly the approximation of dynamic finite elements with mass lumped at the nodes.

In matrix form,

$$[M]\{\ddot{\delta}\} + [K]\{\delta\} = \{R\} \qquad (6)$$

where

$$\{\delta\} = \begin{Bmatrix} UR_1 \\ UZ_1 \\ UR_2 \\ UZ_2 \\ \cdot \\ \cdot \\ \cdot \\ UR_n \\ UZ_n \end{Bmatrix},$$

n is the number of nodes, and the matrix $\{\ddot{\delta}\}$ is a columnar array of nodal acceleration arranged in the same order as $\{\delta\}$.

To solve this set of equations, the accelerations are rewritten in finite difference notation. Thus,

$$\ddot{U}\Big|_{t>0} = \frac{U_{(t + \Delta t)} - 2U_{(t)} + U_{(t - \Delta t)}}{(\Delta t)^2} \tag{7}$$

Substituting the above relation into the equations of motion (6), each equation may be solved algebraically for $U_{(t + \Delta t)}$. The equations are elastically coupled, but this does not interfere with the solution which is done node by node stepwise in time by increments of Δt. The time step Δt can be no larger than the time required for the dilatation wave to cross one element. The elements are right isosceles triangles so $\Delta t_{max} = .707 \frac{DE}{C_1}$, where DE is the length of one leg of the triangle and C_1 is the dilatation wave speed. For convenience $\Delta t = .5 \frac{DE}{C_1}$ was used. This time step produces results indistinguishable from Δt_{max}.

The initial time step is a special case in which the condition

$$\ddot{U}\Big|_{t=0} = \frac{U_{t + \Delta t} - U_{t - \Delta t}}{2\Delta t} = 0 \tag{8}$$

must be used.

CHAPTER III

ACCURACY OF PROGRAM

Ang and Newmark [4] solved a problem involving the blast loading of earth with a finite difference technique. Costantino [5] used the same problem to check his finite element program which used rectangular elements. The program used in this research (Appendix C) used triangular elements (Figure 3) and produced similar results to the previous two solutions. Figure 4 shows the load distribution on the surface. The similarity of the curves in Figure 5 shows each method is satisfactory.

Results from the program in Appendix C were utilized to make Figure 6. The solid lines are theoretical wave positions calculated from the well-known formulas for wave speeds in a solid (see Mason [8]).

$$V_D = \sqrt{\frac{\lambda + 2\mu}{\rho}} \qquad \text{Dilatation wave speed} \qquad (9)$$

$$V_S = \sqrt{\frac{\mu}{\rho}} \qquad \text{Shear wave speed} \qquad (10)$$

where λ and μ are the Lamé constants.

Although the velocities computed are delayed in time, they are correct. The dilatation wave speed was located by the peak compressive axial stress generated by

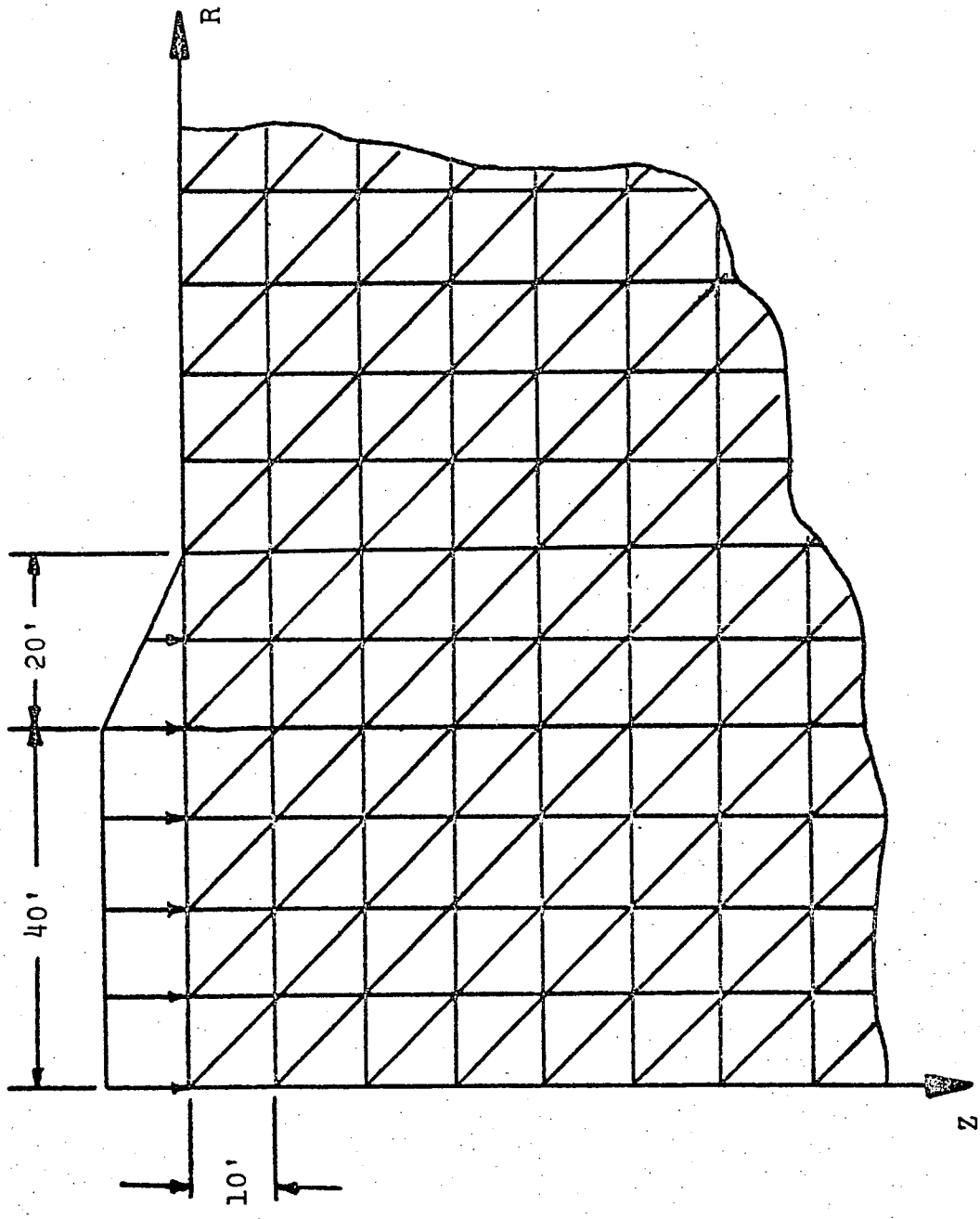

Figure 4. Cross-Sectional View of Grid and Load Distribution for Earth Problem

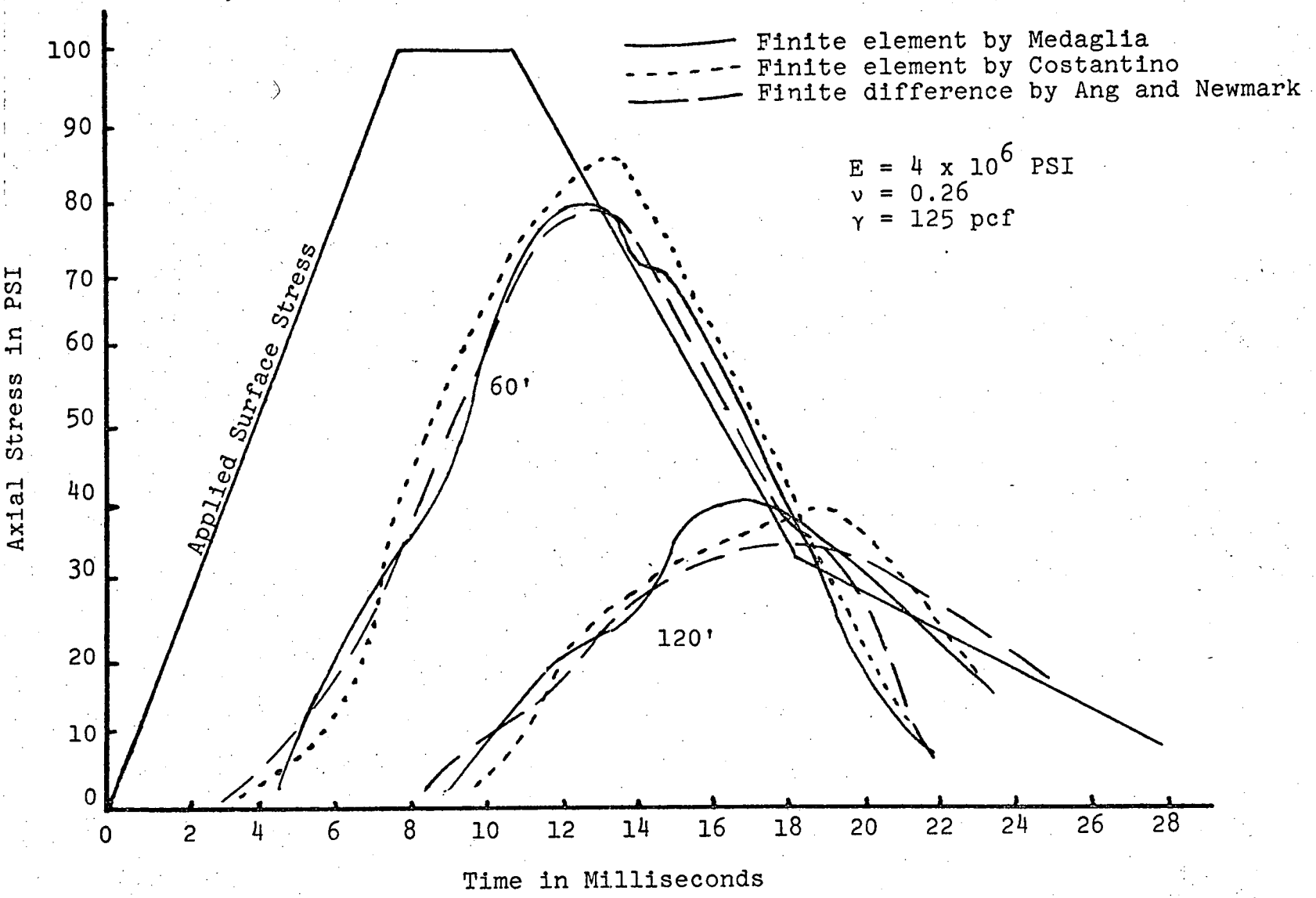

Figure 5. Axial Stress on Centerline of Earth Model

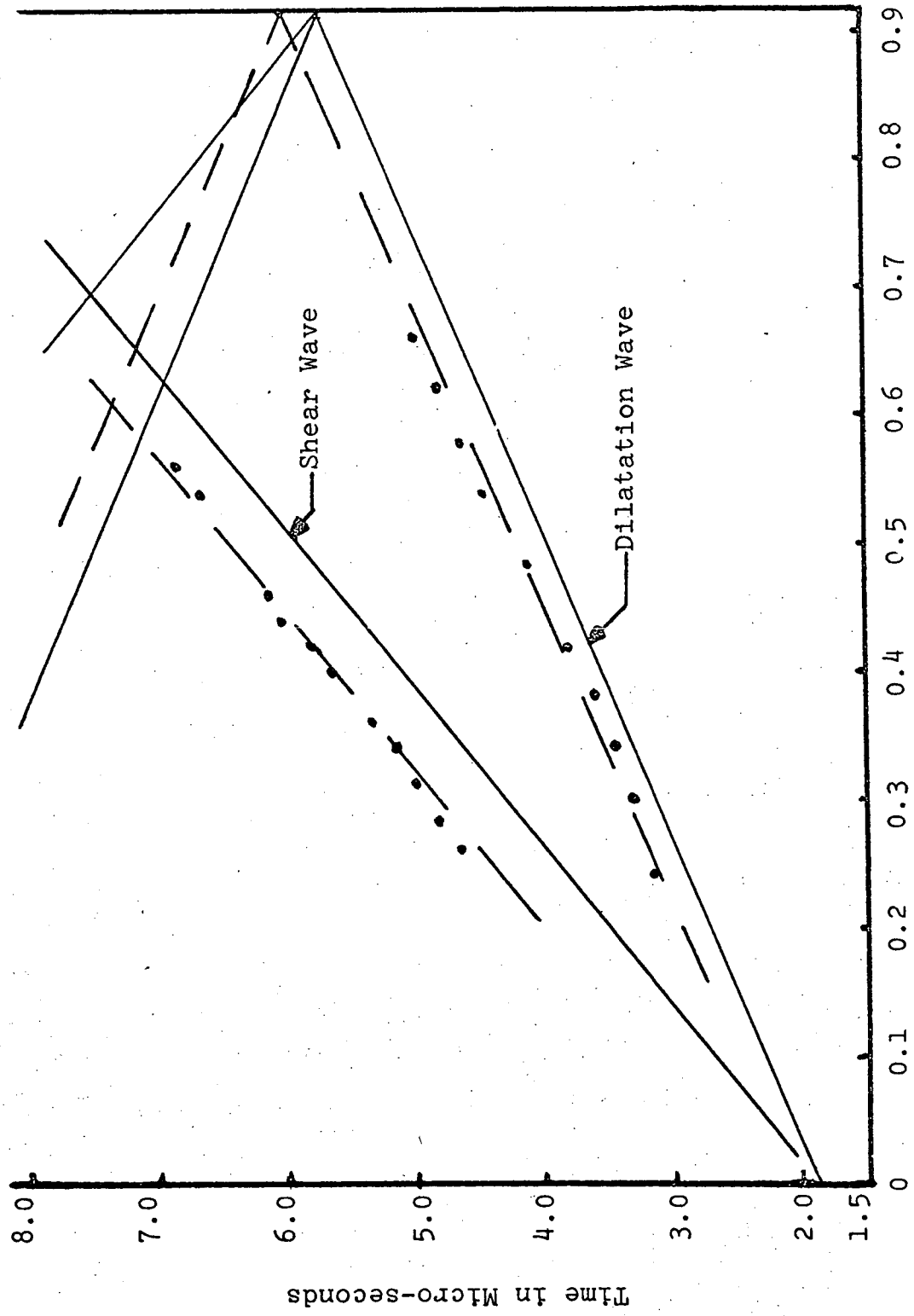

Figure 6. Position of Wave Peaks Produced by Full Sine Pulse Applied as a Point Load

a sinusoidal point load, and the shear wave position was located by the peak radial displacements generated by the same sinusoidal point load. The delay in time is caused by the inertia of the lumped masses resisting the motion imparted by the forcing function. A sample print-out is included in Appendix C.

Figure 7 shows the temporal history of stress at a certain depth on the centerline. The theoretical solution is due to Davids [1]. An exponentially decaying step point load (Figure 8) was applied on the centerline, normal to the surface of the plate. The severe oscillations are due to the element size and the discontinuous nature of the forcing function. The discontinuity was reduced by applying a ramp-step load shown in Figure 9. Davids stated that for a step load the stress at a point would approach a value greater than zero for large times as shown in Figure 10. Figure 10 shows that the longer the ramp time, the smaller the oscillations. In fact it can be seen from Figure 5, that the oscillations become unimportant when the discontinuities in the forcing function are small. When a full sine forcing function is applied, the oscillations are unnoticeable as can be seen in Figure 11. The tensile peak at 1 microsecond is due to the shear wave.

A more precise understanding of the nature of the oscillations may be achieved by writing the finite element equations for a one dimensional bar and solving them by Laplace transforms. This procedure is carried out in detail

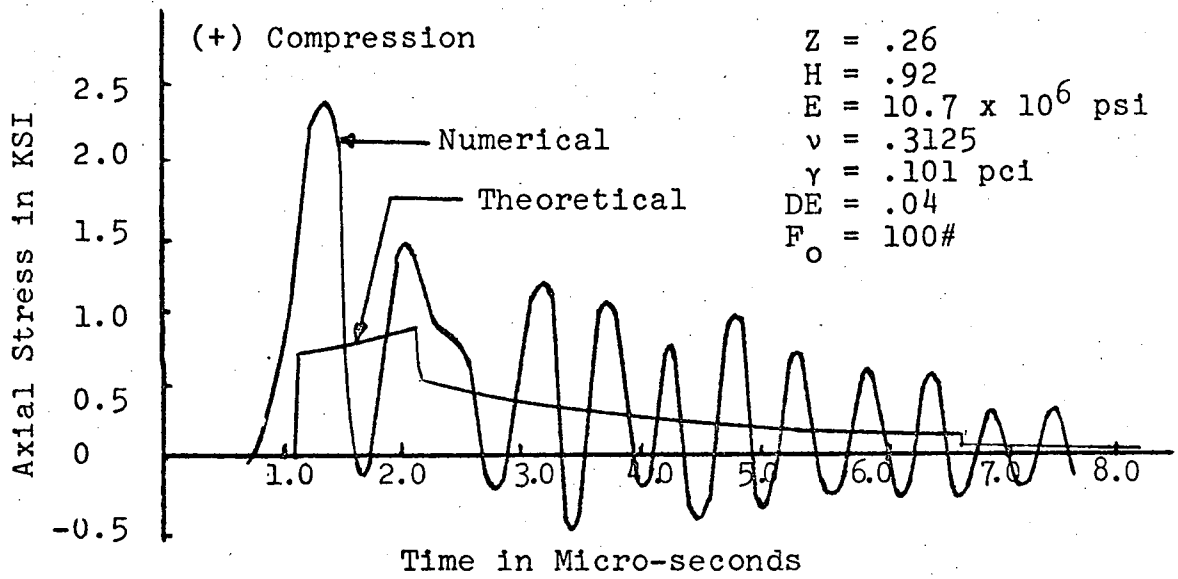

Figure 7. Stress Response at a Point on the Centerline due to an Exponentially Decaying Point Load

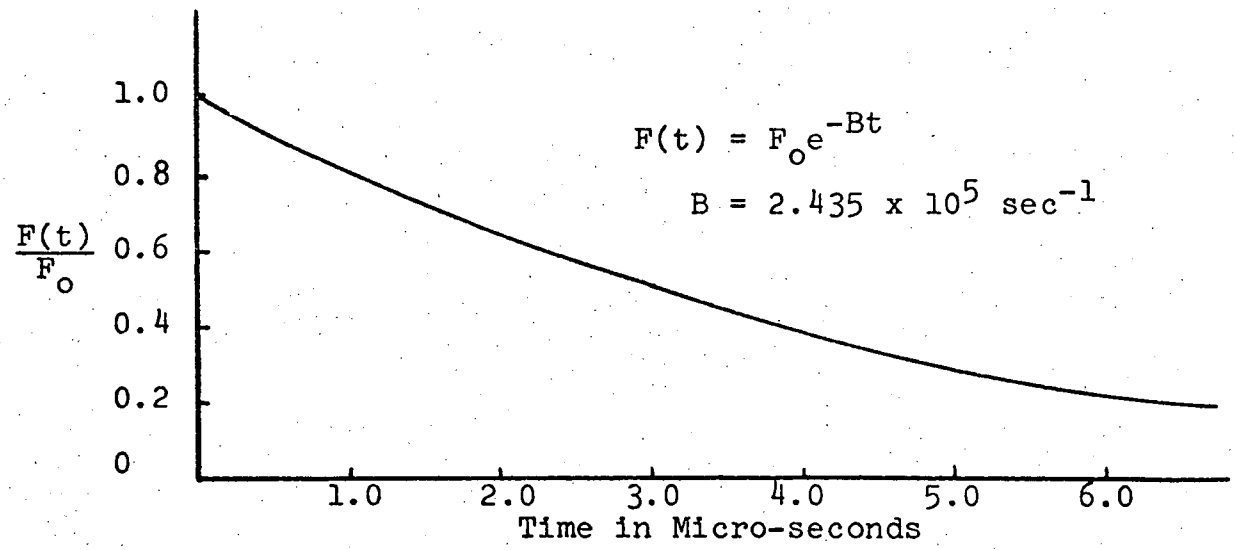

Figure 8. Exponentially Decaying Step Load

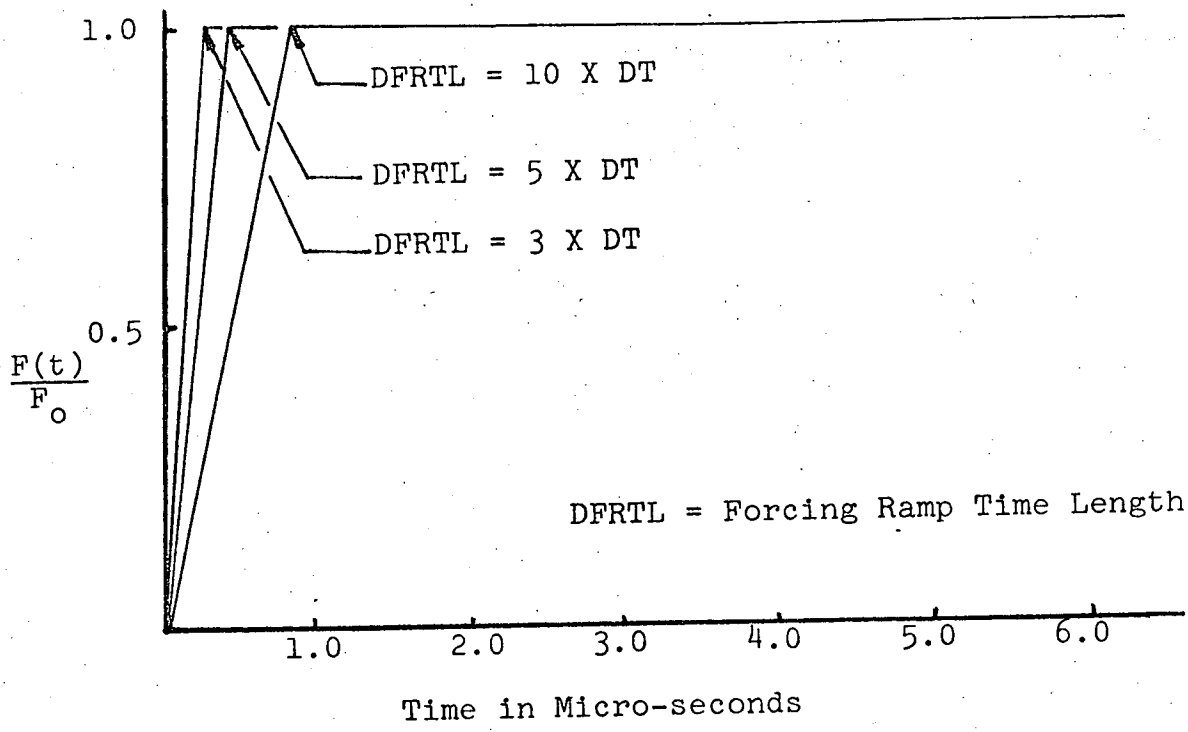

Figure 9. Ramp Step Loads

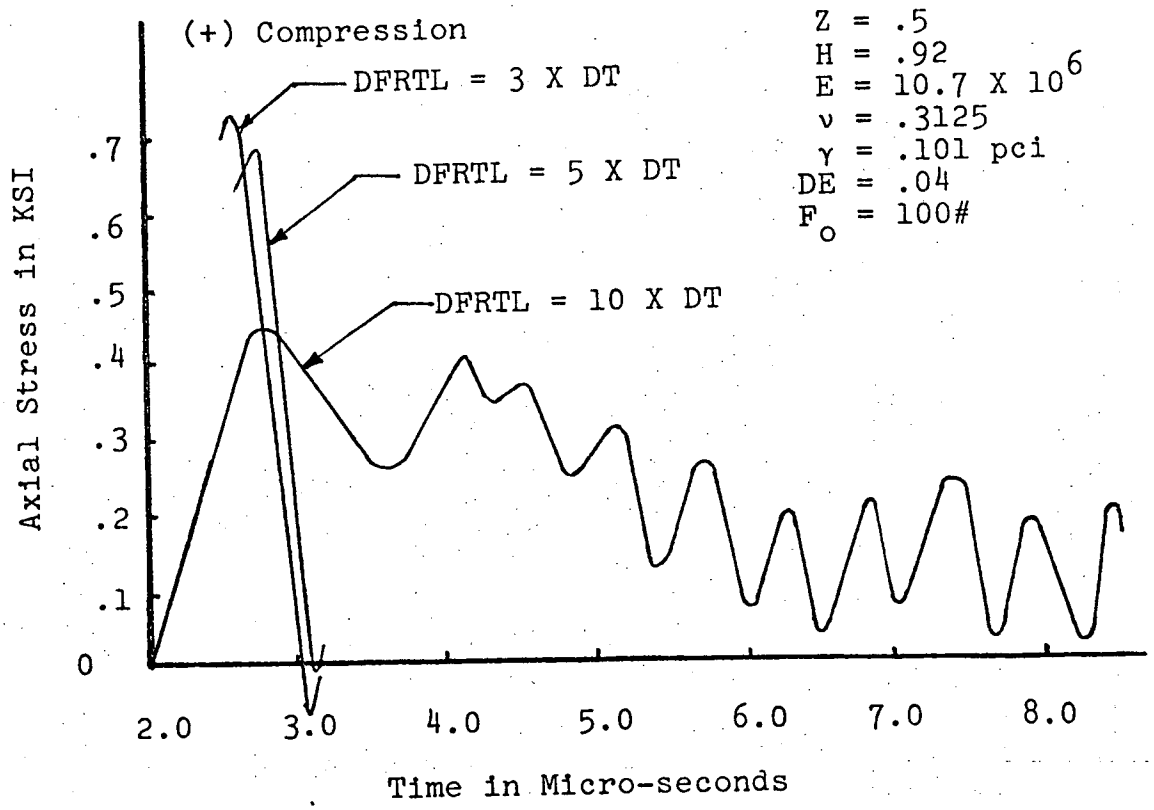

Figure 10. Response to Ramp Step Loads

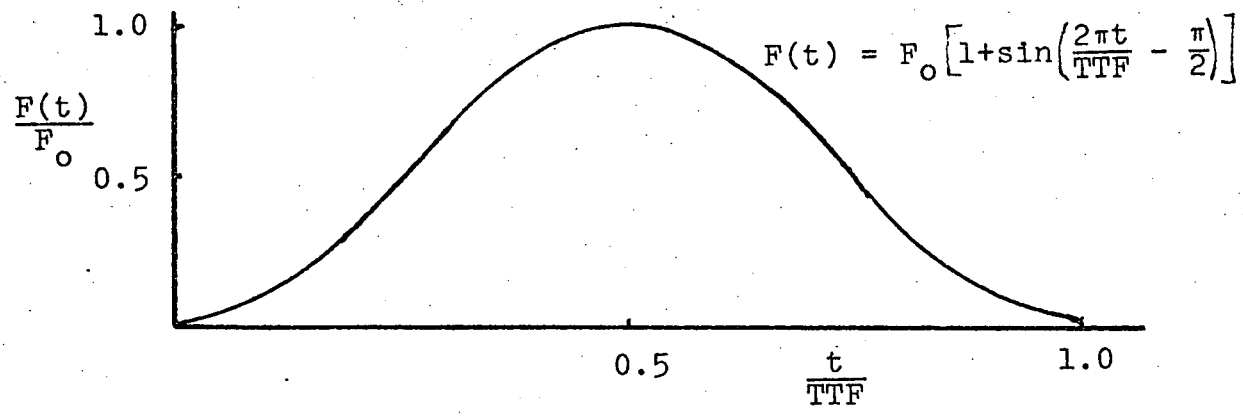

a. Full Sine Pulse

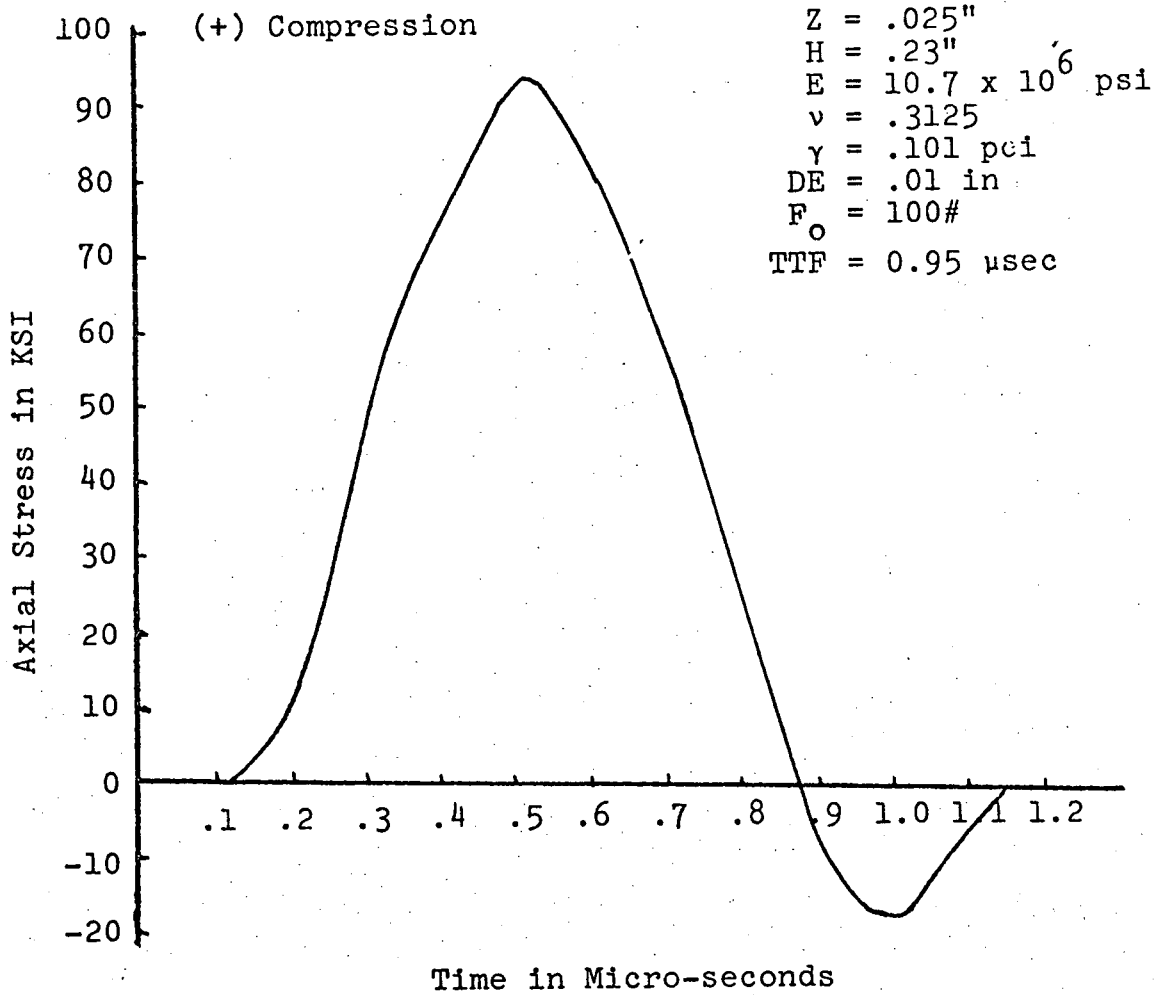

b. Response to Full Sine Pulse Point Load

Figure 11. Full Sine Pulse and Response

in Appendix B. The result is that at time zero for a bar approximated by two elements, using the lumped mass approach the reaction at one end is equal to the applied load at the other end. The same is true when the consistent mass matrix is used. This is because two elements are just one finite difference space for acceleration. For four lumped mass elements, the reaction is one-fifth the applied load. Using four consistent mass elements the reaction equals the applied load at time zero. The exact solution is that the reaction at time zero is zero. The more lumped mass elements that are used, the smaller the reaction. The consistent mass elements always give a reaction equal to the load, no matter how many elements are used, which indicates that the disturbance is propagated at an infinite speed.

The reason for the non-zero (albeit small) reaction in the finite element approximation is that the solution is a Fourier series with a finite number of terms. A plot of such a series is a curve which oscillates about the exact answer. With enough terms in the series, the oscillations become indistinguishable, except at discontinuities. At a discontinuity, a jump known as Gibb's phenomenon always occurs and is proportionate to the size of the discontinuity. The number of finite elements along the length is analagous to the number of terms in a Fourier series for approximation of waves which propagate axially. Therefore, the smaller the element size, the more terms in the series

and the better the approximation. Further, the first term in the series is the mean value of the series, hence the size of the reaction at time zero is just a measure of accuracy.

As a final check of the program, a step load was applied to a long cylindrical bar. Figure 12 shows the results for two element sizes at about the same instant in time. The smaller elements give a more accurate answer in terms of percent error and rapidity of convergence behind the wave front. The small difference in the two results shows the larger element size is actually a good approximation, and the results are influenced strongly by Gibb's phenomenon. The number of nodes in the two problems is equal. The only difference in the two bars is the element size. The grids are identical, each having five nodes radially and 168 nodes axially. The different element size changes the dimensions of the bar, but the number of terms in the approximation is the same. Therefore, the number of terms in the Fourier series for each element size is the same and the accuracy of each should be similar. The series for the smaller elements is somewhat more accurate because the coefficients of the terms in the series are better proportioned.

It is clear from the previous assessment of accuracy that the lumped mass matrix does give satisfactory results with sufficiently small elements and continuous forcing functions. The accuracy improves with finer grids (more

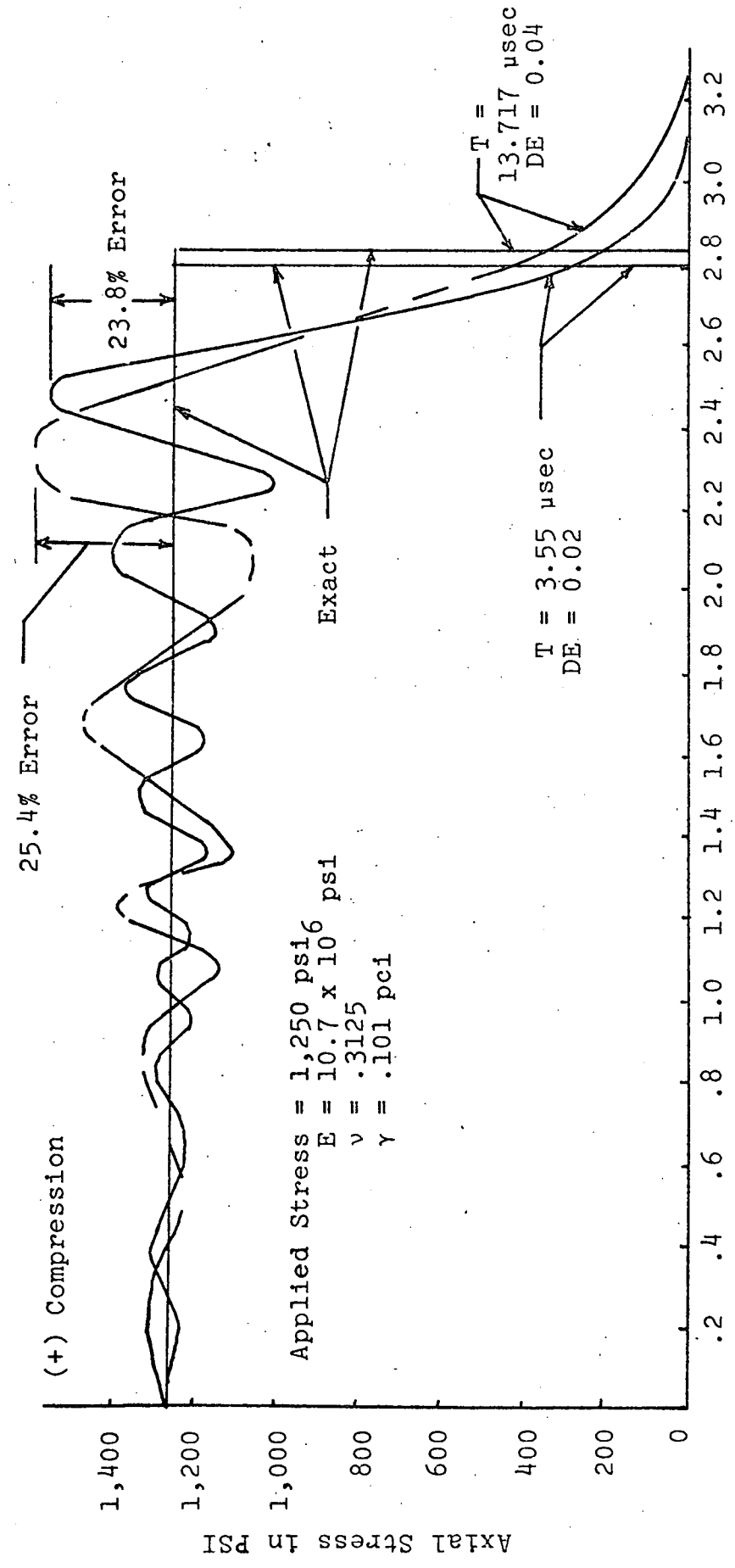

Figure 12. Long Bar Approximated by Two Element Sizes

computer space). While the accuracy of the stresses was limited by the capacity of the computer used, they do compare favorably with other numerical and exact solutions, and the necessary waves are generated at the proper speeds and locations to allow study of spallation. Limitations do exist, however, on the allowable sharpness of a discontinuous input load.

CHAPTER IV

RESULTS

Although all four stresses (radial, circumferential, axial, and shear) are present, examination of the stress distribution has shown that the axial stress is dominant, especially in the area where a fracture may develop. Experimentally produced spalls are usually tensile failures. Since the axial stress is the most prominent, and undergoes the most dramatic fluctuations, and the applied stress is in the axial direction, the results shown are for axial stress. This will serve to illustrate the major response of the plate. It would be futile to attempt to convey all or most of the information generated by the program in the form of graphs. Each problem discussed produced approximately forty stress distributions and nodal displacement displays which were each for separate instant in the response history of the plate. Condensation of these results to comments and a few graphs became essential. Direction of load application was always normal to the front face of the plate.

Point Load

The results of the point load application compare favorably with Davids [1] predictions. Although the step load response oscillates severely for reasons explained in Chapter III and Appendix B, Figure 6 shows the response does follow the proper values in time and space. The response is smooth when a full sine wave is applied as the forcing function (Figure 11).

The full sine forcing function has a shape which produces a clear peak in the response which can be easily followed as the waves propagate. The lack of oscillation and the obvious peak made the full sine forcing function the convenient choice for investigation of the stress waves. For the point load problem, a pulse of 100 pounds maximum amplitude was applied to the centerline in the axial direction. Figure 13 shows the axial stress distribution for several times, and the significant features are labeled.

The stress on the centerline is the only one shown because the magnitude is highest on the centerline. Examination of the semi-graphic printout (see sample printout in Appendix C) showed the stress waves moving out symmetrically from the point of load application in a pattern similar to the ripples produced by a stone dropped in a puddle. Figure 14 shows this pattern in idealized form before and after reflection of the dilatation wave from the back face. Figure 13 shows the response of the plate

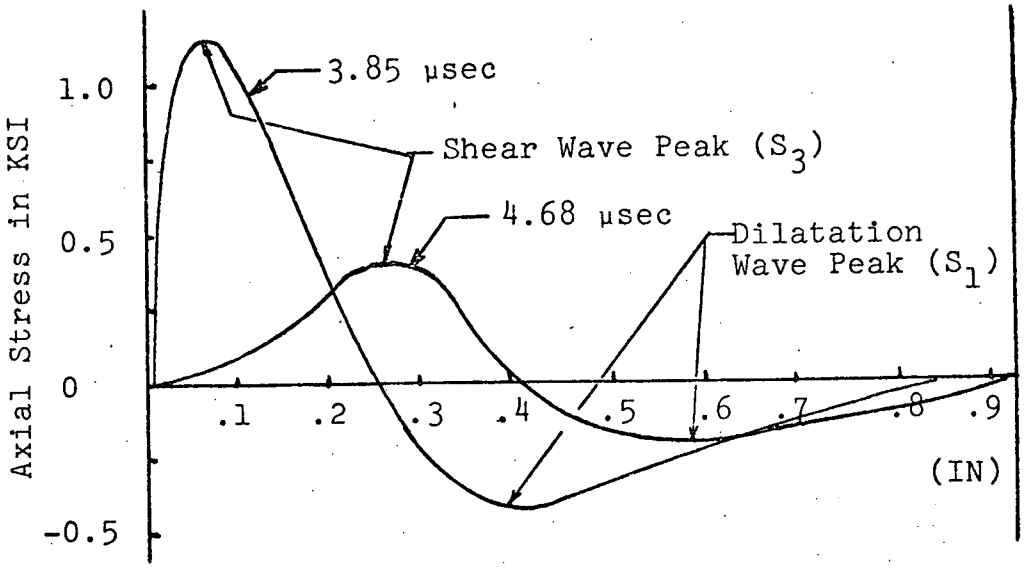

a. Before Reflection of Dilatation Wave

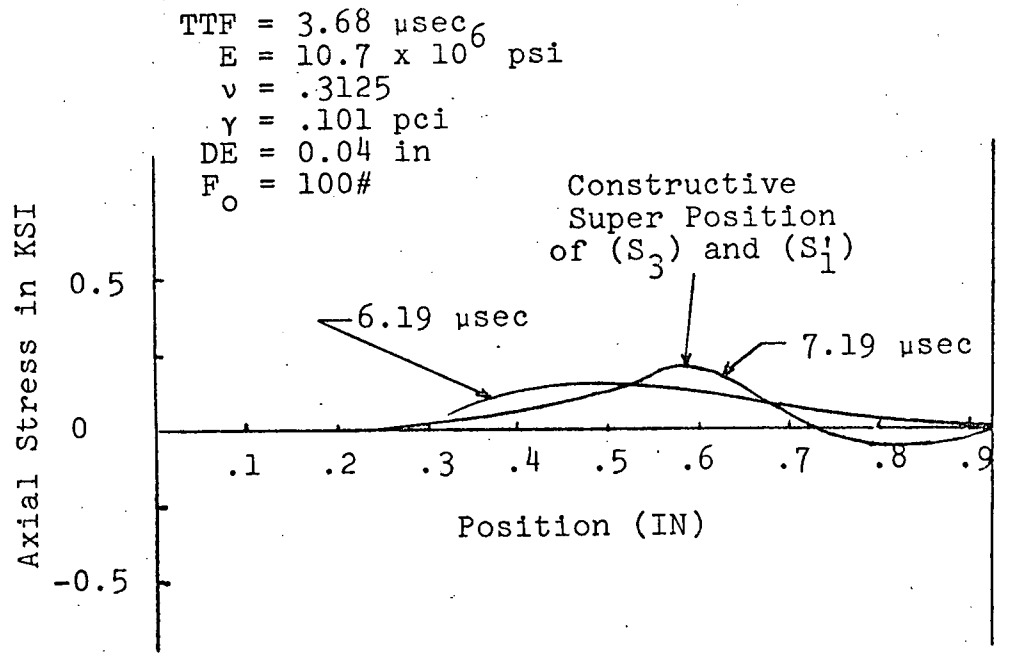

b. After Reflection

Figure 13. Axial Stress on Centerline Caused by Point Load, TTF = 3.68

subjected to a full sine pulse whose period is about the same as the time required for the dilatation wave to cross the thickness of the plate. Figure 15 shows what happens when the period of the pulse is equal to the time required for the dilatation wave to cross five-eighths of the thickness of the plate.

Distributed Load Over a Small Radius

A small radius is one which is equal to or less than about one-third of the plate thickness. The wave initially has a plane front, but seems to round off to a shape like that of the point load and produces a similar response.

The full sine pulse was used for distributed loads, also. A maximum amplitude of 1,000 psi was chosen for convenience.

The wave generated from the front face propagates in the axial direction for radii less than the radius of loading. From the point at the outer edge of the distributed load, the wave moves out like the waves produced by a point load. Since the dilatation wave moves away perpendicularly from the front face, it should not be followed by a shear wave. On the centerline it is not immediately followed by a shear wave.

But at the extreme radius of loading the dilatation wave is followed by a shear wave immediately. It is produced because the dilatation wave has a radial component at that point. As time goes on, the shear wave spreads from the

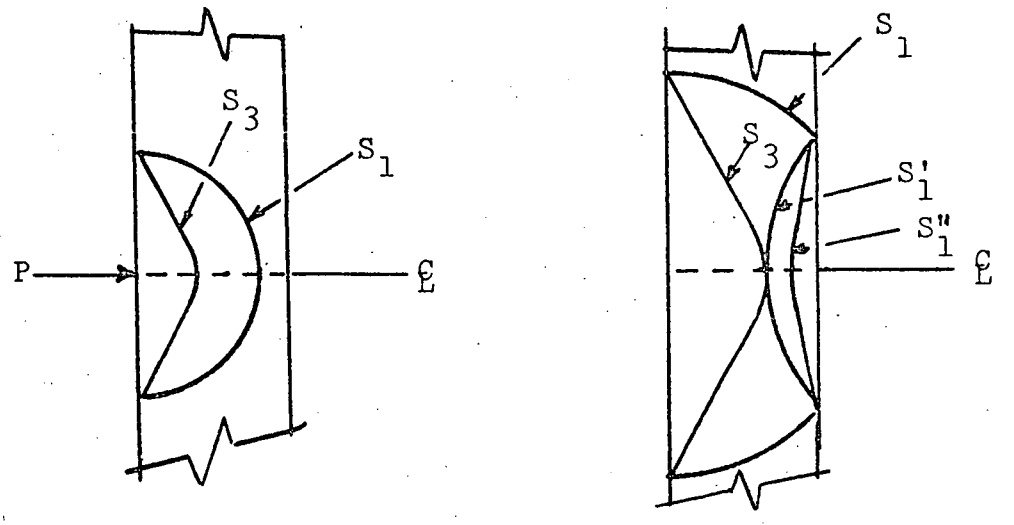

Figure 14. Idealized Wave Patterns Produced by Point Load

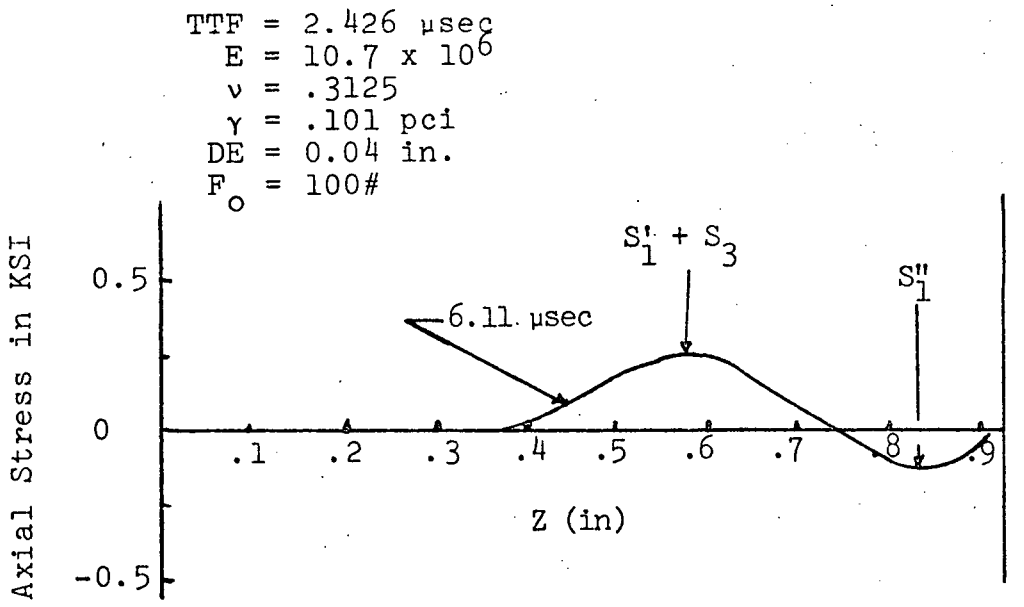

Figure 15. Axial Stress on Centerline Caused by Point Load

TTF = 2.426

radius of loading radially and axially. The radial propagation is actually a radial dilatation wave caused by the Poisson effect. The reflection of this wave from the front face generates the shear wave. With the small radius of loading, the shear wave spreads to the centerline and follows the axial dilatation wave. The smaller the radius of loading, the sooner the shear wave reaches the centerline. In addition, the part of the plane wave at the radius of loading attenuates causing the plane wave to apparently "round-off" to a shape similar to the shape caused by a point load. In comparison to a point load, the shear wave initiation on the centerline is delayed when the load is distributed. Figures 16, 17, 18 and 19 show axial stresses on the centerline for four different radii of loading at different times. Again the centerline is the location of the maximum stress now because of the rounding off of the dilatation wave.

Figure 20 compares the peak axial stress on the centerline as a function of depth for four radii of loading and a point load. The point load decays by the inverse of depth squared. The distributed loads approach a non-decaying plane wave as the radius of loading increases. Figure 21 shows the idealized wave patterns at three times.

Distributed Load Over an Intermediate Radius

An intermediate radius is less than or equal to the plate thickness and greater than one-third of the plate

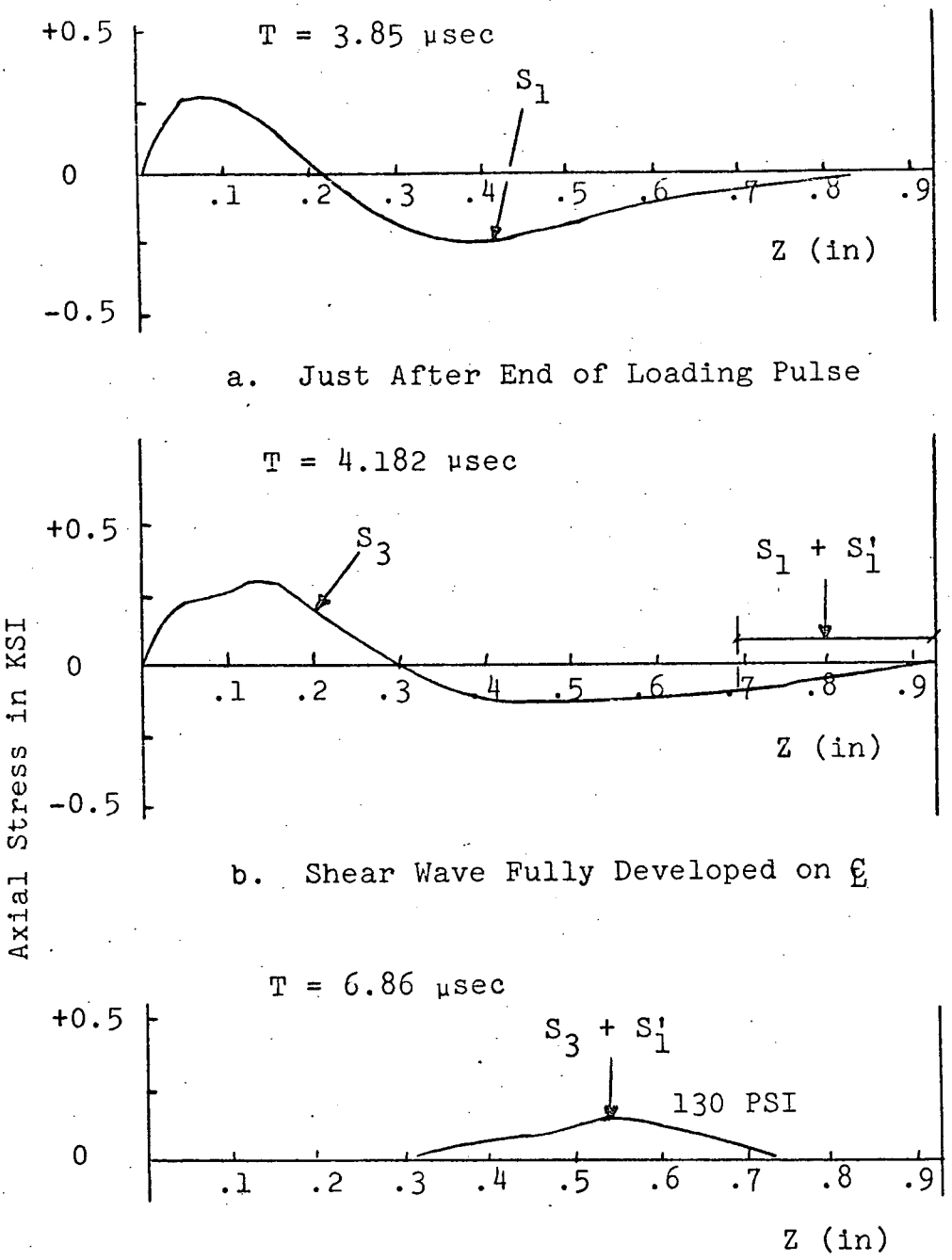

TTF = 3.68 sec
E = 10.7 x 10^6 psi
ν = .3125
γ = .101 pci

DE = 0.04 in.
F_0 = 2,160 psi
a = 0.08 in.

Figure 16. Axial Stress on Centerline Caused by Load over Small Radius, a = 0.08 in.

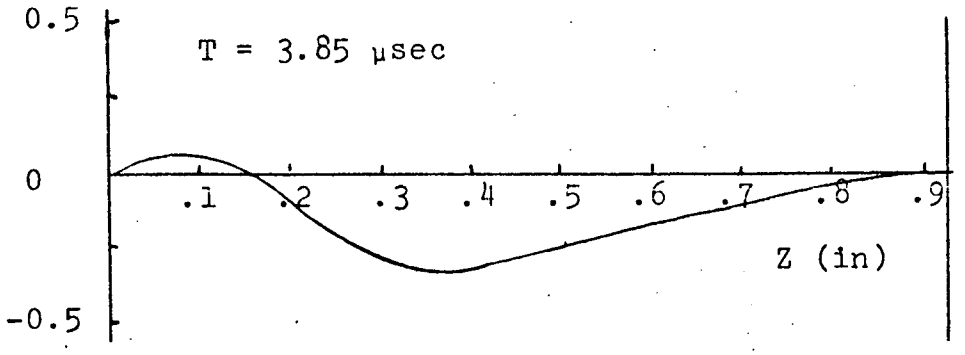

a. Just after End of Loading Pulse

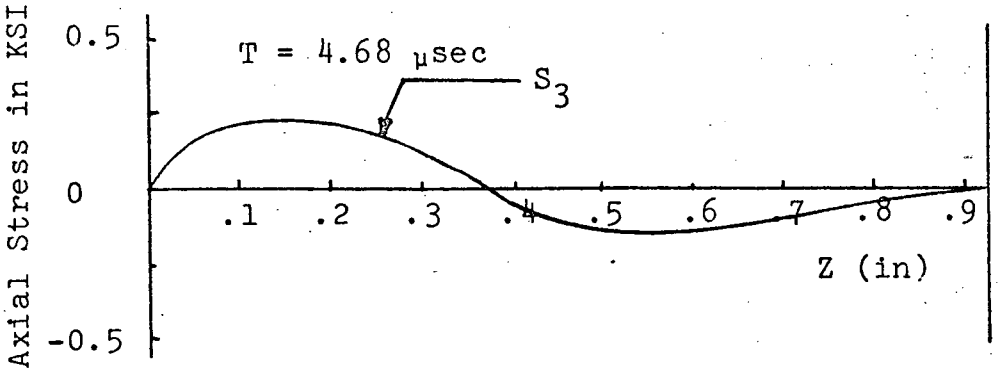

b. Shear Wave Fully Developed on ℄

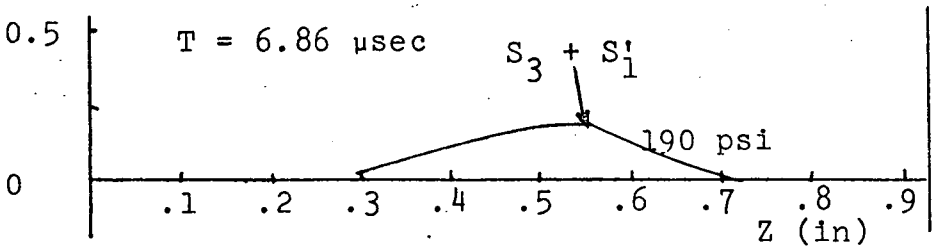

c. Maximum Superposition of $S_3 + S_1'$

TTF = 3.68 μsec
E = 10.7×10^6 psi
ν = .3125
γ = .101 pci

DE = 0.04
F_o = 1,050 psi
a = 0.16 in.

Figure 17. Axial Stress on Centerline Caused by Load Over Small Radius, a = .16 in.

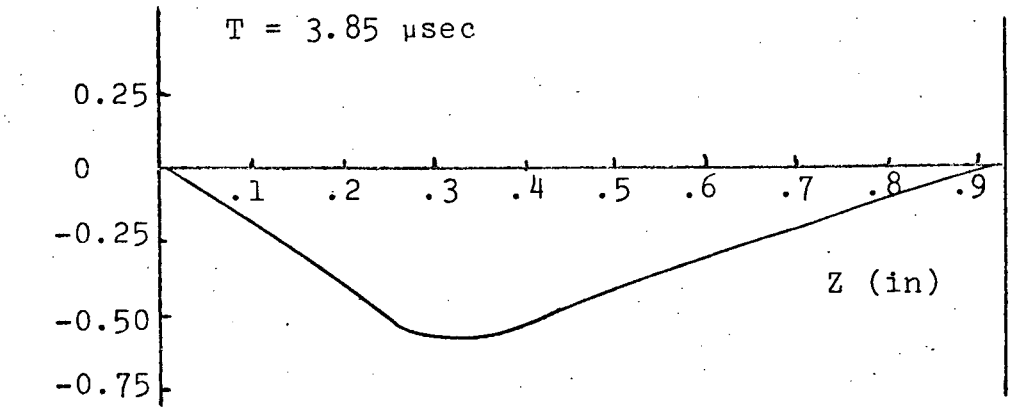

a. Just after End of Loading Pulse

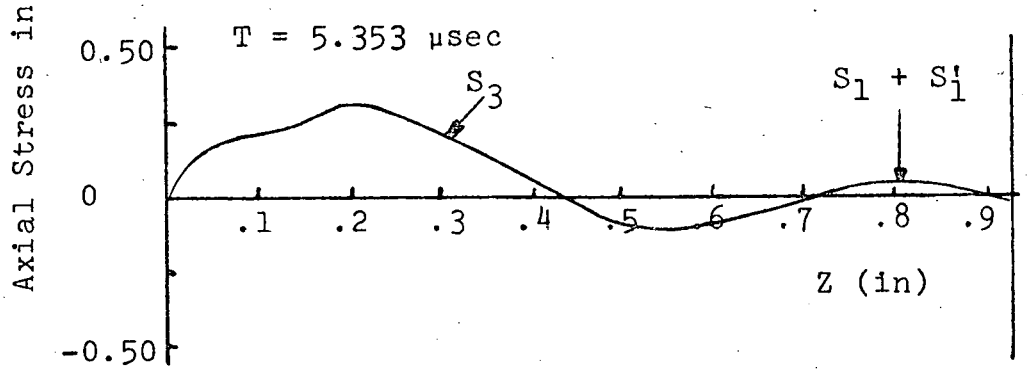

b. Shear Wave Fully Developed on $\mathcal{C}_L$

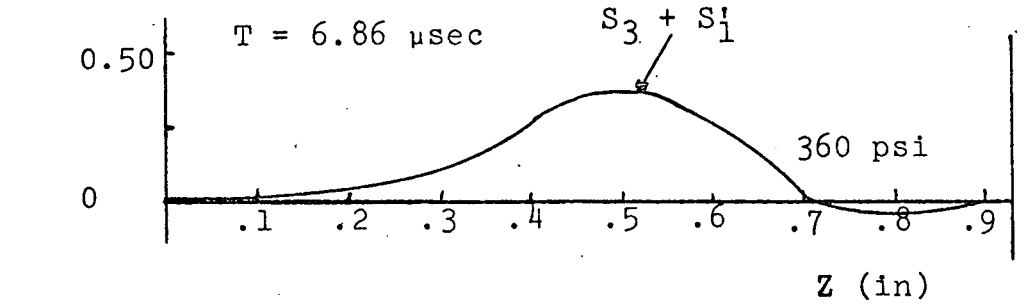

c. Maximum Superposition of $S_3 + S_1'$

TTF = 3.68 μsec
E = 10.7×10^6 psi
ν = .3125
γ = .101 pci

DE = 0.04 in.
F_o = 1,000 psi
a = .24 in.

Figure 18. Axial Stress on Centerline Caused by Load Over Small Radius, a = .24 in.

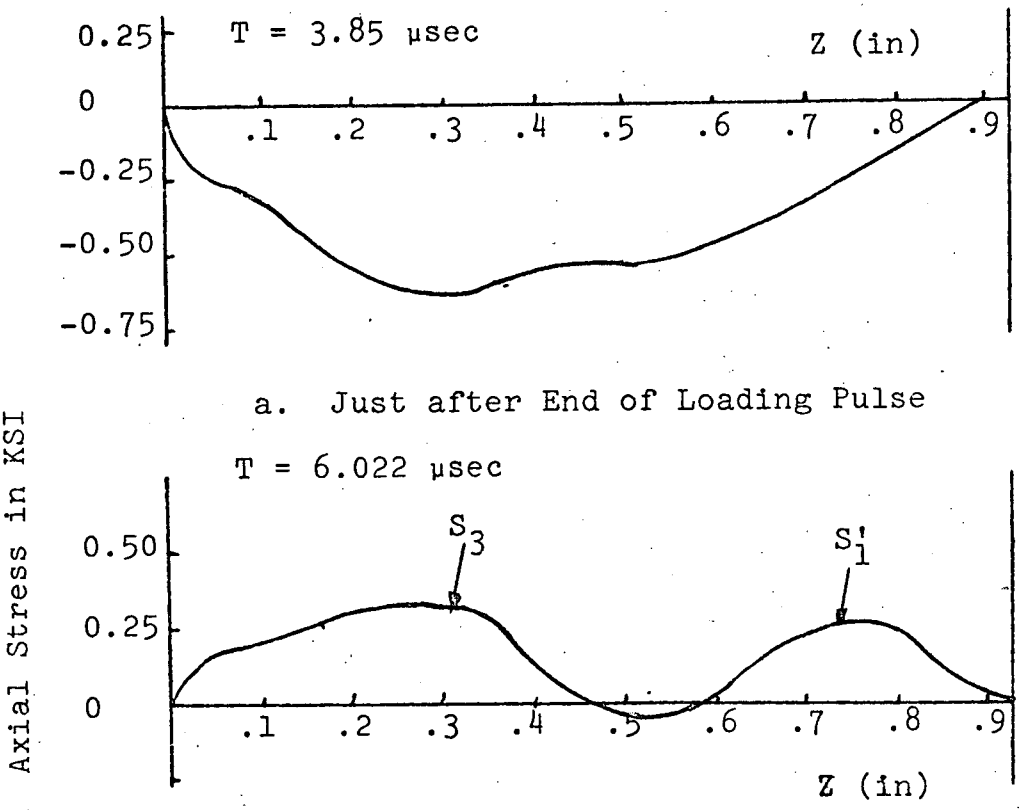

TTF = 3.68 μsec
E = 10.7 X 10^6 psi
ν = .3125
γ = .101 pci

DE = 0.04
F_0 = 1,000 psi
a = .32 in.

Figure 19. Axial Stress on Centerline Caused by Load Over Small Radius, a = .32 in.

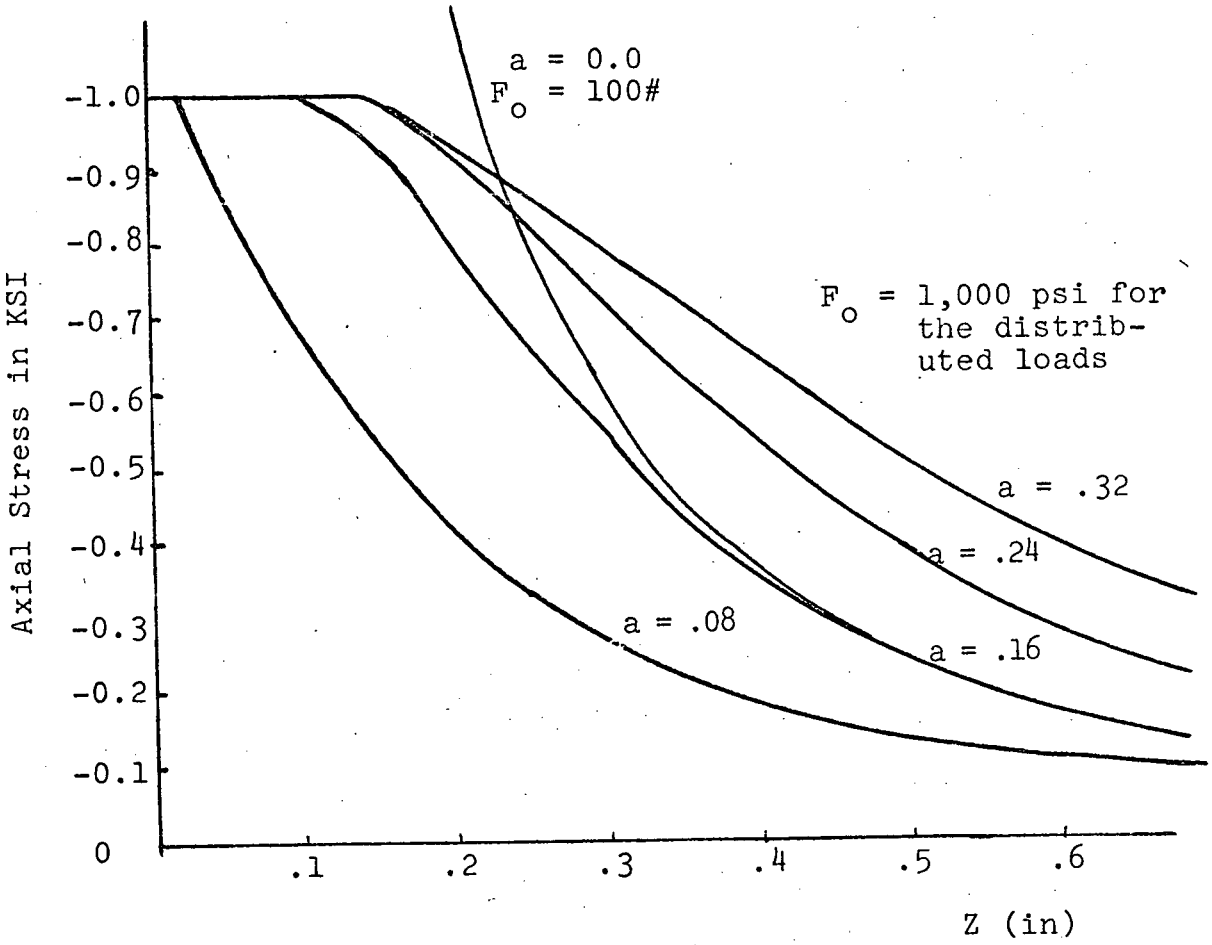

Figure 20. Peak Compressive Axial Stress on Centerline versus Depth

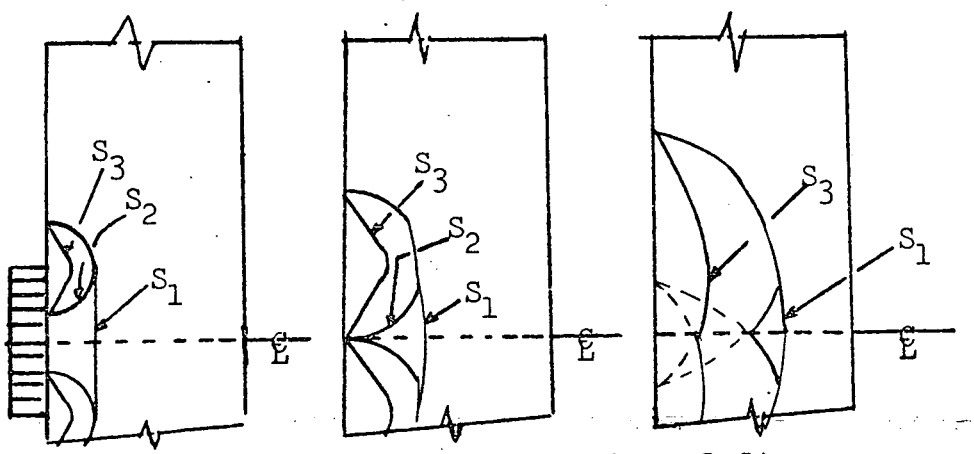

S_2 is an "edge" wave (Ref [2])

Figure 21. Idealized Wave Patterns Produced by Load Over Small Radius

thickness. The maximum axial stress develops on the centerline, but high axial stresses also develop off the centerline.

The high axial stress off the centerline becomes more pronounced as the radius of loading increases. If the axial stress distribution is thought of as a contoured surface, a saddle of lower axial stress exists between the on and off centerline regions of high axial stress.

The on-centerline axial tensile stress develops first. The larger the radius of loading, the closer its location of development approaches a depth of about 70 per cent of the plate thickness. The larger the radius of loading, the deeper the wave on the centerline travels at its applied stress value, resulting in less attenuation and higher peak tensile axial stresses for larger loading radii. The location of this stress buildup corresponds well with the location of the superposition of the edge and dilatation waves. This location is dependent on the wave speeds which are functions of the material properties.

The off-centerline tensile stress increases to a maximum located at a radius less than the loading radius but at a time well after the time the high tensile stress develops on the centerline. At the time the off centerline stress is maximum, it is the greatest tensile stress in the plate, but lower than the previously developed highest stress on the centerline. The location of the off-centerline maximum was observed to occur at half the

loading radius for a loading radius equal to the plate thickness.

Figure 22 shows idealized wave patterns for this case. Figures 23 and 24 show axial stress distribution. Notice that the curves are for radii off the centerline as well as on it. The applied loads were uniform distributed loads.

Distributed Load over a Large Radius

When the loading radius is greater than the plate thickness, the off-centerline tensile axial stress develops first, propagates toward the centerline and exceeds the stress on the centerline. Once it reaches the centerline it continues to increase briefly, then attenuates. It stays on the centerline and propagates toward the front face. While developing and moving toward the centerline, the stress also moves somewhat toward the front face. After it reaches the centerline another "hot-spot" develops off the centerline with lower stresses between it and the centerline. The new hot-spot develops at the same depth as the current maximum centerline stress, moves with it toward the front face and also toward the centerline. This new, late developing hot-spot is smaller than the maximum centerline stress. It is the same as the off centerline hot-spot developed by a load applied over an intermediate radius. Figure 25 shows idealized wave patterns for this case.

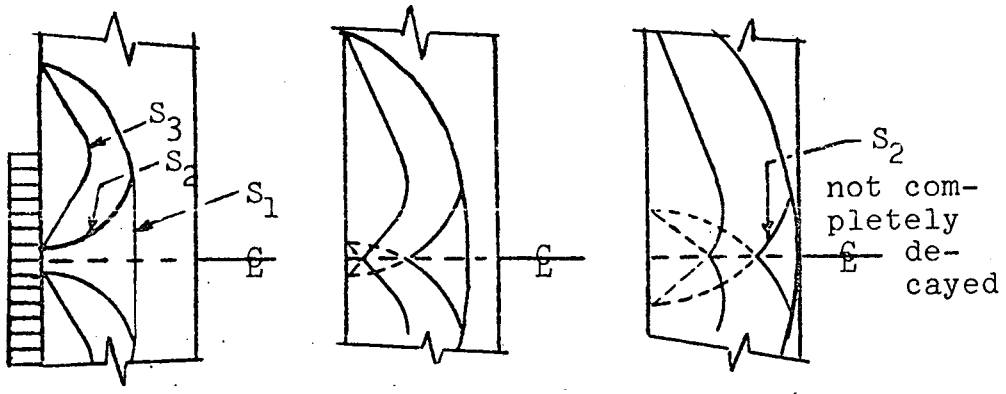

Figure 22. Idealized Wave Patterns for Loading over Intermediate Radius

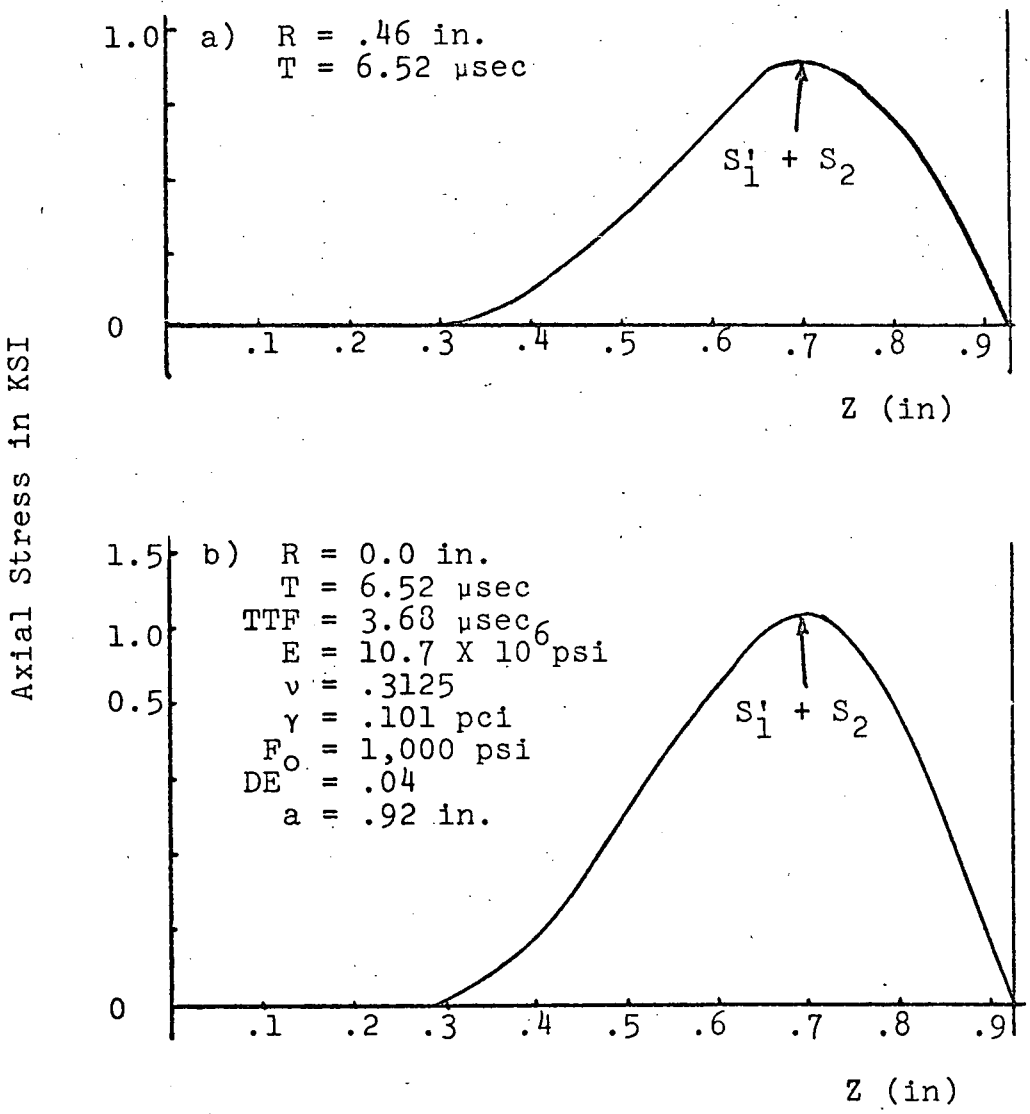

Figure 23. Axial Stresses Due to Load Over Intermediate Radius, T = 6.52 μsec

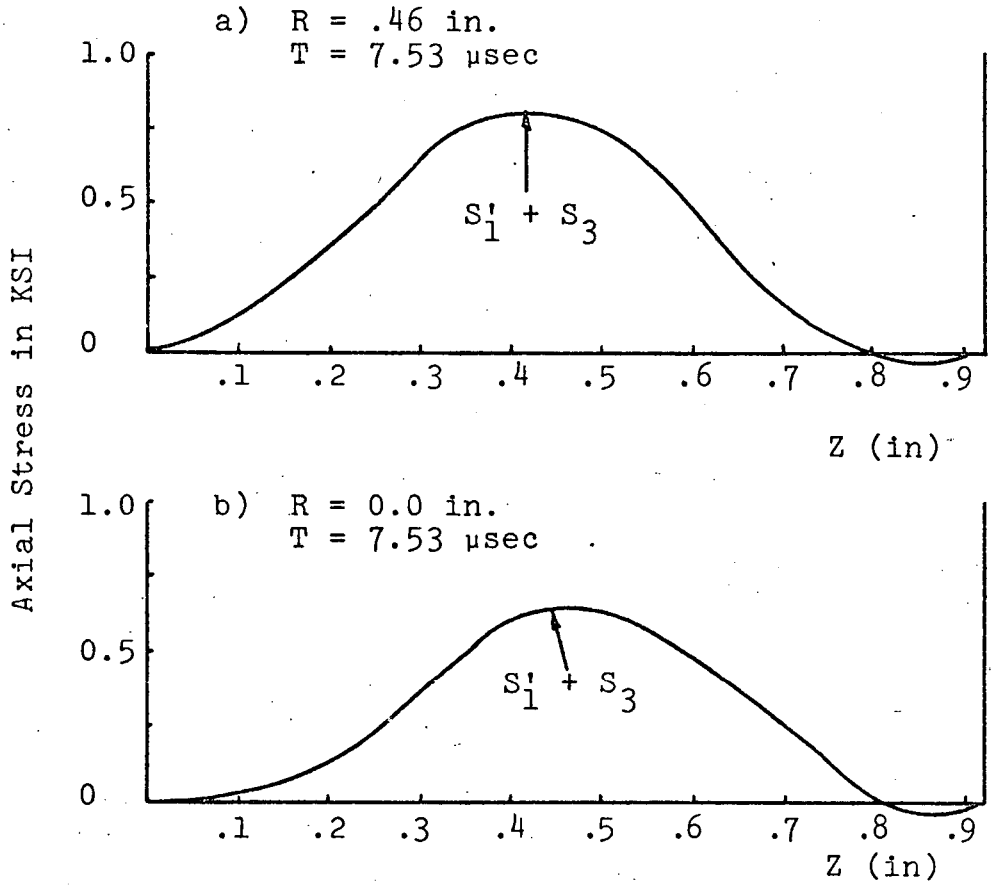

TTF = 3.68 μsec
E = 10.7×10^6 psi
ν = .3125
γ = .101 pci
F_o = 1,000 psi
DE^o = 0.04 in.
a = .92 in.

Figure 24. Axial Stresses due to Load Over Intermediate Radius, T = 7.53 μsec

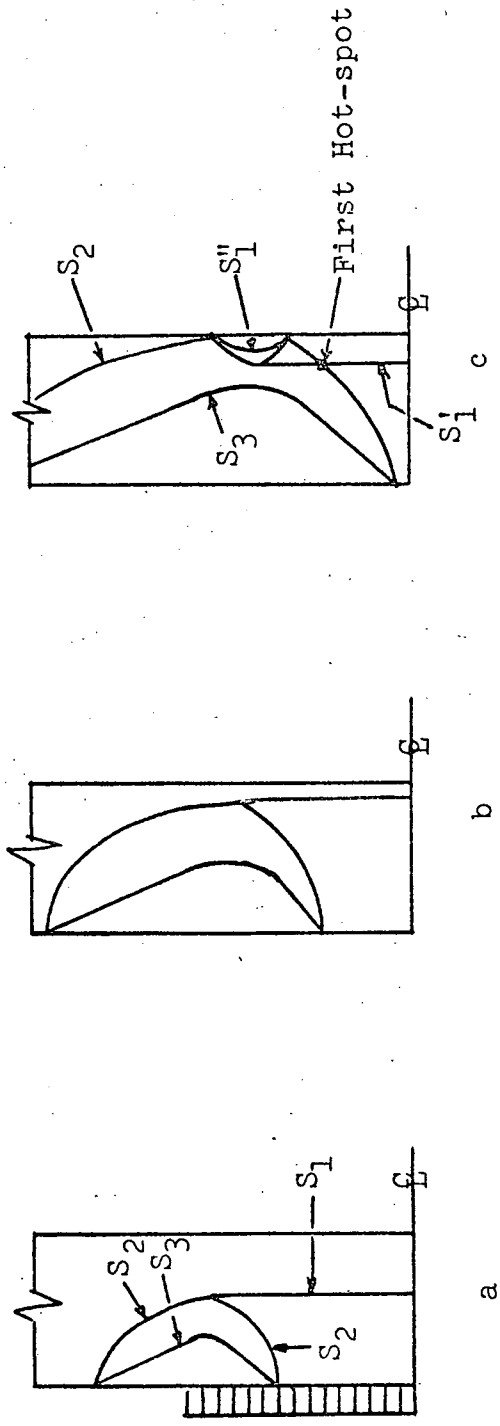

Figure 25. Idealized Wave Patterns for Loading over Large Radius

Figures 26 and 27 show axial stress at different radii and times.

Table 1 shows important stress values, times and locations for each loading condition. Comparison of the times in the last two columns shows whether the maximum stress is due to superposition of the reflected dilatation (S_1') with the incident shear (S_3) or with the edge wave (S_2). The table summarizes several figures in this chapter.

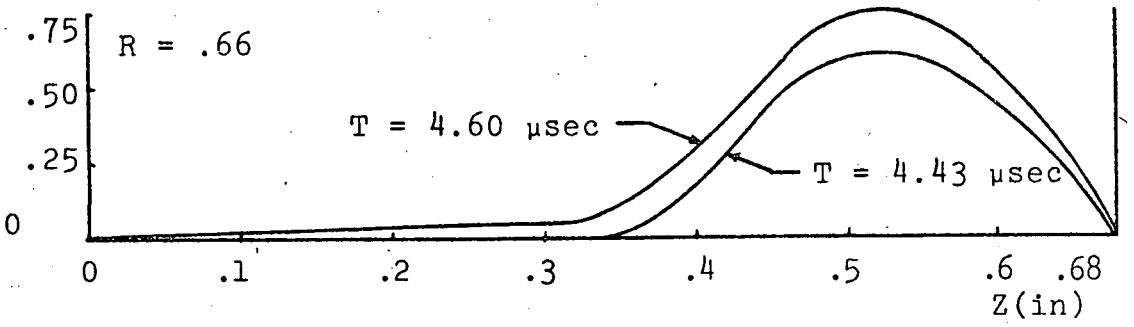

a. Stresses on Radius where Late Hot-spot Occurs

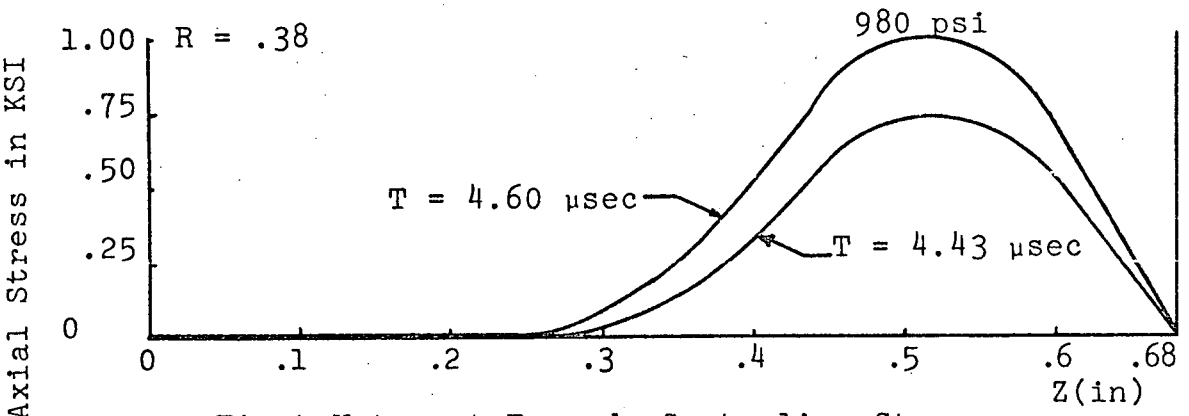

b. First Hot-spot Exceeds Centerline Stress

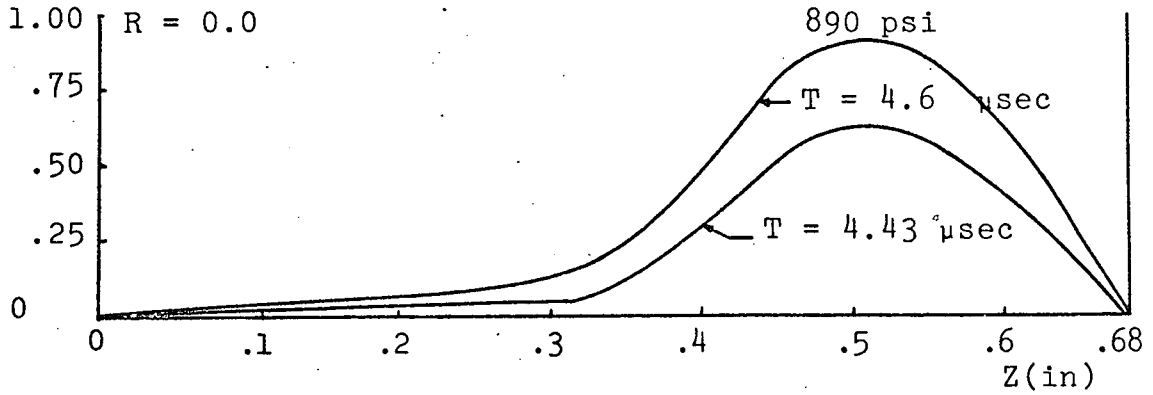

c. Stresses on the Centerline

Figure 26. Axial Stress Caused by Load Over Large Radius, T = 4.43 and 4.60 μsec

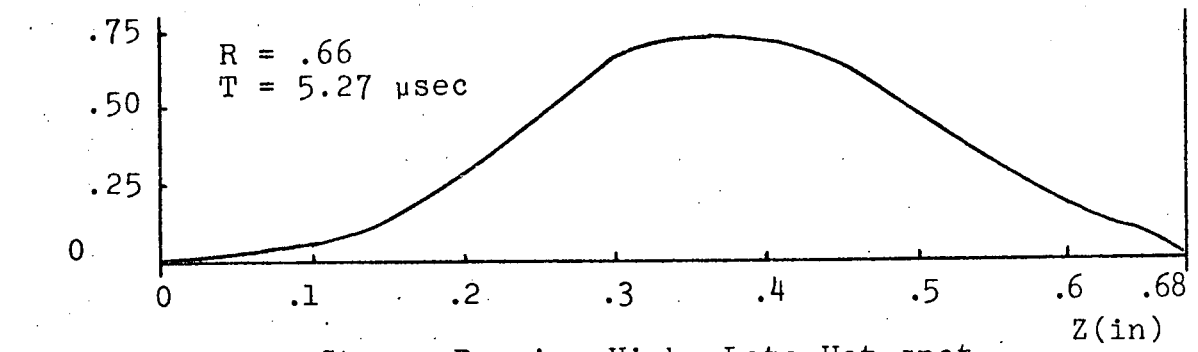

a. Stress Remains High, Late Hot-spot

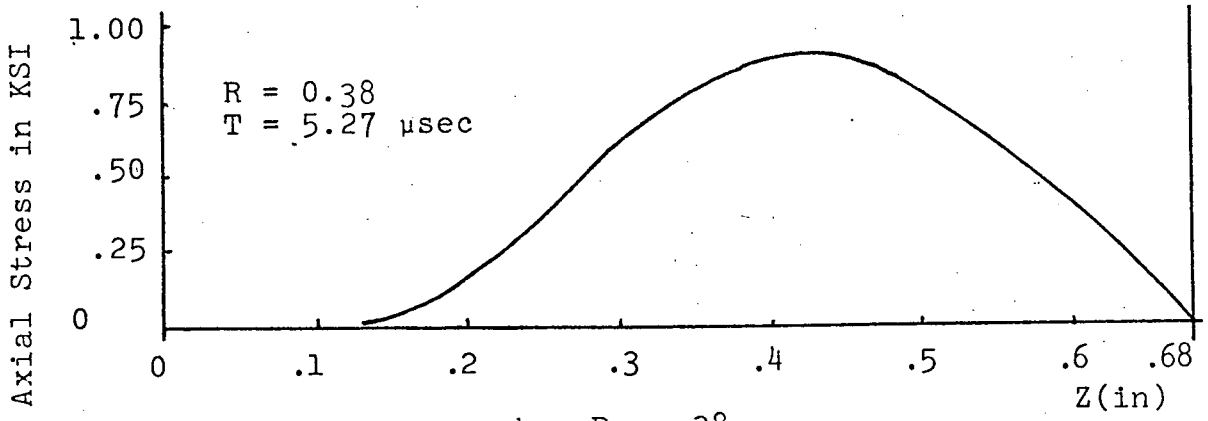

b. R = .38

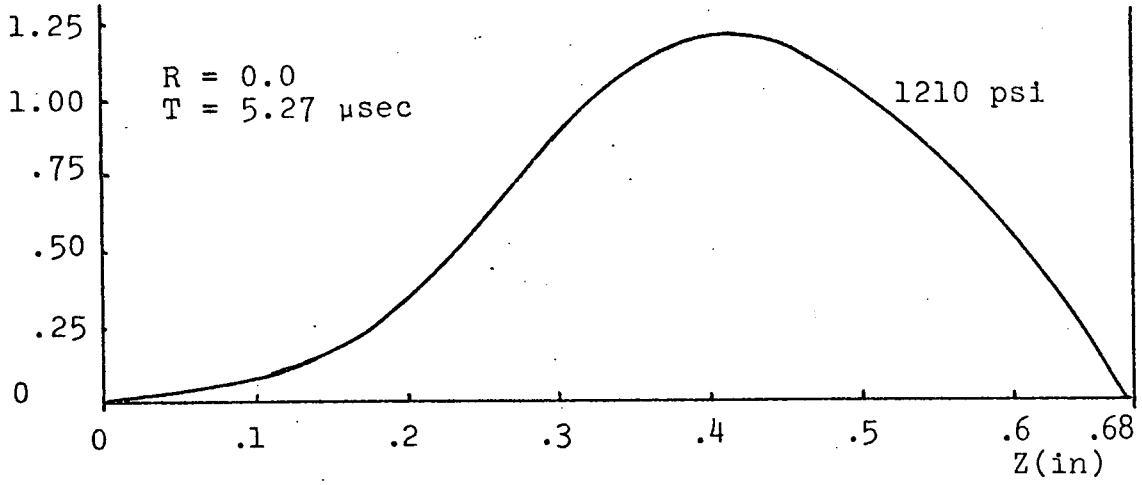

c. First Hot-spot Reaches Centerline

TTF = 2.76 μsec	DE = 0.04
$E = 10.7 \times 10^6$ psi	F_o = 1,000 psi
ν = .3125	a^o = .92 in.
γ = .101 pci	H = .68 in.

Figure 27. Axial Stress Due to Loading Over Large Radius, T = 5.27 μsec

TABLE 1

TIME AND LOCATION OF PEAK AXIAL STRESS

F_o	Load Radius	TTF μsec	Plate Thickness	Axial Stress	Location R	Location Z	Time μsec	Theoretical Time for $S_1' + S_3$
100#	0	3.68	0.92	220 psi	0.0	0.58	7.19	6.9
100#	0	2.43	0.92	260 psi	0.0	0.58	6.11	6.3
2,160 psi	0.08	3.68	0.92	130 psi	0.0	0.54	6.86	6.9
1,000 psi	0.16	3.68	0.92	190 psi	0.0	0.54	6.86	6.9
1,000 psi	0.24	3.68	0.92	360 psi	0.0	0.50	6.86	6.9
1,000 psi	0.32	3.68	0.92	550 psi	0.0	0.54	7.19	6.9
1,000 psi	0.92	3.68	0.92	1,290 psi	0.0	0.70	6.52	6.9
1,000 psi	0.92	3.68	0.92	820 psi	0.46	0.42	7.53	6.9
1,000 psi	0.92	2.76	0.68	980 psi	0.38	0.54	4.60	5.01
1,000 psi	0.92	2.76	0.68	1,210 psi	0.0	0.42	5.27	5.7

CHAPTER V

SUMMARY AND CONCLUSIONS

Detailed, quantitative failure criterion are not discussed in this presentation, but a qualitative discussion is given on the nature of the response of an elastic plate to various impulsive loading conditions.

Point Load

The axial point load on the centerline sends a dilatation wave in all directions, but primarily (in terms of magnitude) in the axial direction. The Poisson effect causes the radial propagation which reflects from the front face as the wave expands. This reflection produces the shear wave, which follows the axial dilatation wave at the shear wave speed. The shear wave has particle motion transverse to the direction of propagation. The dilatation wave has particle motion in the same direction as propagation.

The shear wave produces an axial stress opposite in sign from the axial stress caused by the dilatation wave. When the speedier dilatation wave reflects from the back face (a free surface), the reflection returns at the dilatation wave speed with axial stress of the opposite

sign. The reflection also produces a shear wave, but this shear wave occurs too late to influence spallation. The reflected dilatation wave and incident shear wave, therefore, have axial stress of the same sign and superpose constructively to cause a high tensile stress on the centerline. This high stress can be greater than the tensile strength of the material and lead to a spall. Although the front face may be damaged by the impact or blast, this damage does not necessarily pierce the plate and, until the shear wave and reflected dilatation wave superpose, stresses are not great enough to fracture the material. For a point load, the crack initiates on the centerline and spreads radially. The location on the centerline may be found from graphs similar to Figure 6 for step loads and Dirac delta loading. However, the sine pulse attenuates in a way such that the tensile stress develops at a shallower depth than predicted by Figure 6.

Small, Uniform Loading Radius

Initially, the stress waves differ from the point load, but after the shear wave develops on the centerline, the response is very similar to that of a point loaded plate. The dilatation wave has decayed away from the centerline so it seems to round off, but the front is a straight line radially. This attenuation also occurs on the centerline (after a certain depth) but to a lesser degree. The stress will build up in the same way as for the point

load. The fracture condition develops on the centerline and spreads radially. Attenuation of the sine pulse results in the location of the tensile stress to be at a shallower depth than predicted by Figure 6.

Intermediate Uniform Loading Radius

The dilatation wave front decays inward from the radius of loading until it is "rounded" to the same condition described for a small radius of loading. This occurs before the dilatation wave reflects from the back face and exhibits the same phenomenon which occurred in the waves generated by a uniform load applied over a small radius.

Unlike the case of the small loading radius, a "hot-spot" of tensile stress develops off the centerline at a position and time indicating the cause is superposition of incident shear and reflected dilatation waves. However, this hot-spot develops late and is smaller than the stress which develops on the centerline.

The stress on the centerline results from the combination of the reflected dilatation wave and the incident wave labeled S_2 in Figure 25 (see discussion for large loading radius). It develops on the centerline because the dilatation wave has attenuated away from the centerline. Therefore, the fracture develops on the centerline and propagates outward. A secondary crack may develop off the centerline if the hot-spot has a high enough tensile value.

Large Uniform Loading Radius

The numerical results from a large loading radius clearly support the mathematical analysis of Viswanathan and Biswas [2]. The highest tensile stress develops off the centerline before a high tensile stress develops on the centerline. Also, it develops too early to be caused by combination of the shear wave and reflected dilatation wave. It moves toward the centerline while moving toward the front face. It does not develop until after reflection of the dilatation wave. These conditions mean that the reflected dilatation wave is combining with what Viswanathan and Biswas call "an edge wave . . . with a toroidal front, expanding with velocity c," the dilatation wave speed. Figure 25 shows this "edge wave" labeled "S_2." "Edge" refers to the outer edge of the loaded area on the front face, from which the edge wave emanates. Therefore the crack initiates off the centerline and propagates toward it. The location of the off-centerline tensile stress development is at a radius less than the radius of loading due to the same attenuation "round-off" described earlier.

The stress on the centerline may exceed the tensile strength of the material before the off-centerline crack gets there. A second crack would develop on the centerline and travel outward to meet the first crack in this case.

Finally, it should be noted that attenuation of the wave resulted in the four cases described. If the wave front had maintained the input stress between the centerline

and radius of loading, only the two cases of point load and distributed load need have been discussed. Without attenuation even the smallest of loading radii would produce the highest stress off the centerline first due to superposition of S_1' and S_2. This would occur near to the back face and at the radius of loading. The shape of the waves does not attenuate or round-off. The magnitude does attenuate from the radius of loading (least attenuation on the centerline), making the waves seem to round-off. The reason for this attenuation may be thought of as a "diffusion" of stress from the highly stressed (saturated) region inside the radius of loading to the region outside the radius of loading where the plate has low stresses. This diffusive process is due to the Poisson effect which causes wave propagation in directions other than the direction of loading.

BIBLIOGRAPHY

1. Davids, Norman, "Transient Analysis of Stress-Wave Penetration in Plates," Journal of Applied Mechanics, December, 1959.

2. Viswanathan, K., and Rathindra Nath Biswas, "Analysis of Stress-Wave Penetration in Plates," Indian Journal of Pure and Applied Mathematics, Vol. I, October, 1970.

3. Dally, J. W., and Riley, W. F., "Stress Wave Propagation in a Half Plane Due to a Transient Point Load," Developments in Theoretical and Applied Mechanics, III, Proc. 3rd Southeastern Conference on Theory and Applied Mechanics, University of South Carolina, 1966.

4. Ang, A., and Newmark, N. M., "Computation of Underground Structural Response," Report No. DASA 1376, University of Illinois for Defense Atomic Support Agency, Washington, D.C., June, 1963.

5. Costantino, Carl J., "Finite Element Approach to Stress Wave Problems," Journal of the Engineering Mechanics Division, Proc. of the A.S.C.E., April, 1967.

6. Zienkiewicz, O. C., The Finite Element Method in Engineering Science; McGraw-Hill, 1971.

7. Fung, Y. C., A First Course in Continuous Mechanics, Prentice-Hall, 1969.

8. Mason, Physical Acoustics and the Properties of Solids, D. Van Nostrand, 1958.

9. Biot, M. A., and von Kármán, T., Mathematical Methods in Engineering, 1st ed., McGraw-Hill, 1940.

APPENDICES

DO NOT PRINT

APPENDIX A

APPENDIX A

DERIVATION OF FINITE ELEMENT MATRICES

Displacement Functions

The displacements within elements are given by:

$$UR = \alpha_1 + \alpha_2 R + \alpha_3 Z$$
$$UZ = \alpha_4 + \alpha_5 R + \alpha_6 Z \qquad (A.1)$$

where R and Z are the coordinates of the point whose displacement is being calculated. UR and UZ are the radial and axial displacements, respectively. Since the displacement functions are valid for the nodes as well as inside the element, the unknown coefficients α_1 through α_6 may be determined by writing the displacement functions at each node. Let the nodes and elements of the system be numbered in the manner of Figure 3. Let the nodes of each element be i, j and m in a counter-clockwise manner and refer to the global numbers of Figure 3.

$$
\begin{aligned}
UR_i &= \alpha_1 + \alpha_2 R_i + \alpha_3 Z_i \\
UR_j &= \alpha_1 + \alpha_2 R_j + \alpha_3 Z_j \\
UR_m &= \alpha_1 + \alpha_2 R_m + \alpha_3 Z_m \\
UZ_i &= \alpha_4 + \alpha_5 R_i + \alpha_6 Z_i \\
UZ_j &= \alpha_4 + \alpha_5 R_j + \alpha_6 Z_j \\
UZ_m &= \alpha_4 + \alpha_5 R_m + \alpha_6 Z_m
\end{aligned}
\tag{A.2}
$$

The constants α_1 , α_2 , and α_3 may be solved from the first three equations by Cramer's rule and α_4 , α_5 , and α_6 are found in the same way from the last three equations. One example and other results follow.

$$
\alpha_1 = \frac{\begin{vmatrix} UR_i & R_i & Z_i \\ UR_j & R_j & Z_j \\ UR_m & R_m & Z_m \end{vmatrix}}{\begin{vmatrix} 1 & R_i & Z_i \\ 1 & R_j & Z_j \\ 1 & R_m & Z_m \end{vmatrix}}
\tag{A.3}
$$

Solving A.3 gives:

$$
\alpha_1 = \frac{(a_i UR_i + a_j UR_j + a_m UR_m)}{(a_i + a_j + a_m)}
\tag{A.4}
$$

where $(a_i + a_j + a_m) = 2A$ = twice the area of the triangle. Similarly the other α's are defined in terms of nodal

displacements. The arithmetic terms a, b, and c are defined in Table 2.

$$\alpha_1 = \frac{(a_i UR_i + a_j UR_j + a_m UR_m)}{2A}$$

$$\alpha_2 = \frac{(b_i UR_i + b_j UR_j + b_m UR_m)}{2A}$$

$$\alpha_3 = \frac{(c_i UR_i + c_j UR_j + c_m UR_m)}{2A} \qquad (A.5)$$

$$\alpha_4 = \frac{(a_i UZ_i + a_j UZ_j + a_m UZ_m)}{2A}$$

$$\alpha_5 = \frac{(b_i UZ_i + b_j UZ_j + b_m UZ_m)}{2A}$$

$$\alpha_6 = \frac{(c_i UZ_i + c_j UZ_j + c_m UZ_m)}{2A}$$

TABLE 2

COEFFICIENTS USED IN THE DEFINITION OF DISPLACEMENT

$a_i = (R_j Z_m - R_m Z_j)$	$b_i = (Z_j - Z_m)$	$c_i = (R_m - R_j)$
$a_j = (R_m Z_i - R_i Z_m)$	$b_j = (Z_m - Z_i)$	$c_j = (R_i - R_m)$
$a_m = (R_i Z_j - R_j Z_i)$	$b_m = (Z_i - Z_j)$	$c_m = (R_j - R_i)$

Strain-Displacement Relations

The definition of strain in terms of displacement for axisymmetric problems is:

$$\begin{aligned}
\varepsilon_R &= \frac{\partial UR}{\partial R} = \alpha_2 \\
\varepsilon_\theta &= \frac{UR}{R} = \frac{\alpha_1}{RBAR} + \alpha_2 + \frac{\alpha_3 ZBAR}{RBAR} \\
\varepsilon_Z &= \frac{\partial UZ}{\partial Z} = \alpha_6 \\
\gamma_{RZ} &= \frac{\partial UR}{\partial Z} + \frac{\partial UZ}{\partial R} = \alpha_3 + \alpha_5
\end{aligned} \tag{A.6}$$

The definition of ε_θ includes the following approximation since these are constant strain elements.

$$\begin{aligned}
RBAR &= \frac{(R_i + R_j + R_m)}{3} \\
ZBAR &= \frac{(Z_i + Z_j + Z_m)}{3}
\end{aligned} \tag{A.7}$$

Define the element displacement matrix as:

$$\{\delta\}_e = \begin{Bmatrix} UR_i \\ UZ_i \\ UR_j \\ UZ_j \\ UR_m \\ UZ_m \end{Bmatrix} \tag{A.8}$$

Substitution of the definitions of the constants, α_i, results in the strain displacement equations in matrix form. Equations A.6 become:

$$\begin{Bmatrix} \varepsilon_R \\ \varepsilon_\theta \\ \varepsilon_Z \\ \gamma_{RZ} \end{Bmatrix} = \frac{1}{2A} \begin{bmatrix} b_i & 0 & b_j & 0 & b_m & 0 \\ d_i & 0 & d_j & 0 & d_m & 0 \\ 0 & c_i & 0 & c_j & 0 & c_m \\ c_i & b_i & c_j & b_j & c_m & b_m \end{bmatrix} \{\delta\} \qquad (A.9)$$

where:

$$d_i = \frac{a_i}{RBAR} + b_i + \frac{c_i ZBAR}{RBAR}$$

$$d_j = \frac{a_j}{RBAR} + b_j + \frac{c_j ZBAR}{RBAR} \qquad (A.10)$$

$$d_m = \frac{a_m}{RBAR} + b_m + \frac{c_m ZBAR}{RBAR}$$

The Stiffness Matrix

The element stiffness was derived on page 10 to be:

$$[K]_e = 2 \cdot \pi \cdot RBAR \cdot A[B]^T[D][B] \qquad (A.11)$$

In order to develop a procedure for assembling the stiffness matrix for many elements, consider a two element example, shown in Figure 28.

For the system, equilibrium of nodal forces gives:

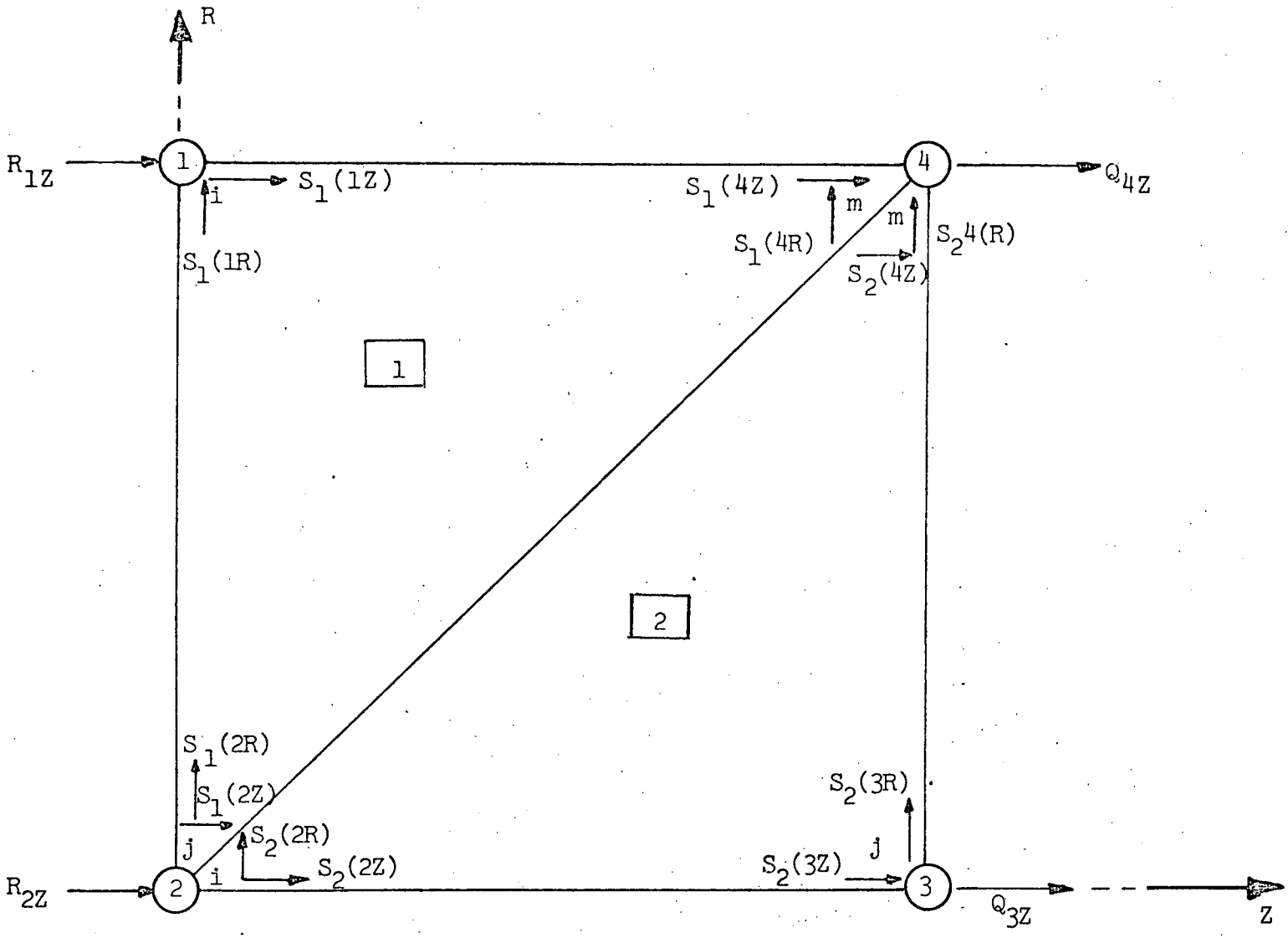

Figure 28. Two Element Example

$$
\begin{aligned}
S_1(1R) &= 0 \\
S_1(2Z) &= R_{1Z} \\
S_1(2R) + S_2(2R) &= 0 \\
S_1(2Z) - S_2(2Z) &= R_{2Z} \\
S_2(3R) &= 0 \\
S_2(3Z) &= Q_{3Z} \\
S_2(4R) + S_2(4R) &= 0 \\
S_2(4Z) + S_2(4Z) &= Q_{4Z}
\end{aligned}
\qquad \text{(A.12)}
$$

Notation: $S_1(1R)$

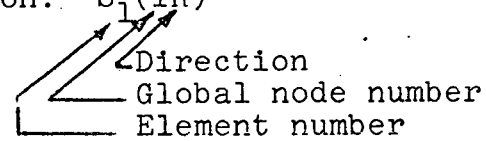

The element stiffness equilibrium equations define the nodal forces (S) in terms of stiffness times displacement. Substitution of these terms in the above system equilibrium equations results in the assembled stiffness matrix for the two element system. In order to show that the position of the element stiffness term in the assembled stiffness matrix is given by node number, the element stiffness matrices for the two element example are given in the equations below in expanded form. The program in Appendix B uses the same minimum space (KELM) for each element stiffness matrix and in the subroutine KFORM computes the positions to add them to in the assembled stiffness matrix (KASY) by node number and a pointer matrix (NADJ). Maximum

storage compression is achieved by using NADJ to eliminate the zero terms in a row, resulting in KASY having only fourteen columns.

$$[K]_1\{\delta\} + [K]_2\{\delta\} = \{R\} \tag{A.13}$$

$$[K]_1 = \begin{bmatrix} k_{11}^{(11)} & k_{12}^{(12)} & 0 & k_{13}^{(14)} \\ k_{21}^{(21)} & k_{22}^{(22)} & 0 & k_{23}^{(24)} \\ 0 & 0 & 0 & 0 \\ k_{31}^{(41)} & k_{32}^{(42)} & 0 & k_{33}^{(44)} \end{bmatrix} \tag{A.14}$$

$$[K]_2 = \begin{bmatrix} 0 & 0 & 0 & 0 \\ 0 & k_{11}^{(22)} & k_{12}^{(23)} & k_{13}^{(24)} \\ 0 & k_{21}^{(32)} & k_{23}^{(33)} & k_{24}^{(34)} \\ 0 & k_{31}^{(42)} & k_{32}^{(43)} & k_{33}^{(44)} \end{bmatrix} \tag{A.15}$$

$$\{\delta\} = \begin{Bmatrix} UR_1 \\ UZ_1 \\ UR_2 \\ UZ_2 \\ UR_3 \\ UZ_3 \\ UR_4 \\ UZ_4 \end{Bmatrix} \qquad \{R\} = \begin{Bmatrix} 0 \\ R_{1Z} \\ 0 \\ R_{2Z} \\ 0 \\ Q_{3Z} \\ 0 \\ Q_{4Z} \end{Bmatrix} \tag{A.16}$$

Each k in the above expanded element stiffness matrices (A.14 and A.15) is a 2 by 2 partition of the original 6 by 6 element stiffness matrix. The subscript refers to the row and column position of the partition in the 6 by 6 element stiffness matrix. The superscript is determined by the i, j, m node numbers of the element and is the position of the partition in the assembled stiffness matrix. This is further illustrated below. Consider any one element with some external loading (R).

$$[K]_e\{\delta\}_e = \{R\} \tag{A.17}$$

$$\begin{array}{c} \\ i \\ j \\ m \end{array} \begin{array}{c} \begin{array}{ccc} i & j & m \end{array} \\ \begin{bmatrix} k_{11} & k_{12} & k_{13} \\ k_{21} & k_{22} & k_{23} \\ k_{31} & k_{32} & k_{33} \end{bmatrix} \end{array} \begin{Bmatrix} \delta_i \\ \delta_j \\ \delta_m \end{Bmatrix} = \begin{Bmatrix} R_i \\ R_j \\ R_m \end{Bmatrix} \tag{A.18}$$

where δ_i , R_i , etc., are 2 by 1 partitions such that:

$$\delta_i = \begin{Bmatrix} UR_i \\ UZ_i \end{Bmatrix} \quad \text{and so forth.}$$

The system of forcing KELM to conform to the i, j, m sequence of nodal displacements in the $\{\delta\}_e$ array insures that the proper indexing of the partition will occur.

The Lumped Mass Matrix

The lumped mass matrix is computed by the subroutine MFORM. Since the grid generated by this program is regular and defined by the number of nodes axially and radially, the mass matrix is formed node by node. The nature of the grid (Figure 3) allows the matrix to be computed in stages, as indicated by the comment cards (see Appendix C). For example, all interior nodes are shared by six elements, so the factor CF is equal to 2. The average of the radii to the centroids (RBAR's) of the six elements surrounding any interior node is always the same as the radius of the node, so DR = 0 . Similarly the mass lumped at each node is based on the number of elements which share the node and the average of the radii to the centroids of those elements. The lumped mass matrix for the two element example in Figure 28 is:

$$[M] = \begin{bmatrix} .333\rho AC_1 & 0 & 0 & 0 & 0 & 0 & 0 & 0 \\ 0 & .333\rho Ac_1 & 0 & 0 & 0 & 0 & 0 & 0 \\ 0 & 0 & .667\rho Ac_2 & 0 & 0 & 0 & 0 & 0 \\ 0 & 0 & 0 & .667\rho Ac_2 & 0 & 0 & 0 & 0 \\ 0 & 0 & 0 & 0 & .333\rho Ac_3 & 0 & 0 & 0 \\ 0 & 0 & 0 & 0 & 0 & .333\rho Ac_3 & 0 & 0 \\ 0 & 0 & 0 & 0 & 0 & 0 & .667\rho Ac_2 & 0 \\ 0 & 0 & 0 & 0 & 0 & 0 & 0 & .667\rho Ac_2 \end{bmatrix} \quad (A.12)$$

where,

c_1 = RBAR for element 1

$c_2 = R_{1Z} - R_{2Z}$

c_3 = RBAR for element 2.

DO NOT PRINT

APPENDIX B

APPENDIX B

DERIVATION OF LUMPED AND CONSISTENT MASS MATRICES FOR ONE DIMENSIONAL PROBLEM WITH LAPLACE TRANSFORM SOLUTION

Description of Problem

In order to determine which mass matrix approach should be used for propagation problems, both will be used to generate equations approximating a bar subjected to a step tensile load at the free end and fixed at the other end. Laplace transformation will be the method of solution of the equations resulting in an expression for the fixed end reaction at $t = 0(+)$. One dimensional finite elements are used to approximate the bar which is assumed to have a length many times greater than the diameter.

Lumped Mass Matrix

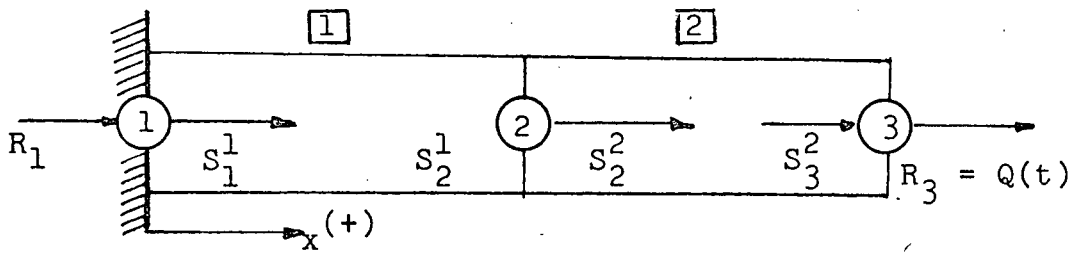

The subscript refers to the node and the superscript refers to the element. Let an element be described in general as follows and choose a linear displacement function.

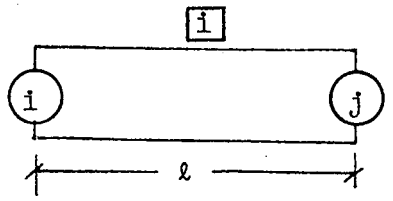

A = area

E = Young's modulus

ρ = mass density

$$u = \alpha_1 + \alpha_2 x \tag{B.1}$$

$$\varepsilon_x = \alpha_2 = \frac{u_j - u_i}{\ell} \tag{B.2}$$

$$[B] = \frac{1}{\ell}[-1 \quad 1] \tag{B.3}$$

$$[D] = [E] \tag{B.4}$$

$$\{\delta\}_e = \begin{Bmatrix} u_i \\ u_j \end{Bmatrix}, \{\delta\} = \begin{Bmatrix} u_1 \\ u_2 \\ u_3 \end{Bmatrix}, \{\ddot{\delta}\} = \begin{Bmatrix} \ddot{u}_1 \\ \ddot{u}_2 \\ \ddot{u}_3 \end{Bmatrix} \tag{B.5}$$

$$[K]_e = A\ell[B]^T[D][B] \tag{B.6}$$

$$[K]_e = \frac{AE}{\ell}\begin{bmatrix} 1 & -1 \\ -1 & 1 \end{bmatrix} \tag{B.7}$$

$$\{\delta\}_e = [K]_e\{\delta\}_e \tag{B.8}$$

$$
\begin{aligned}
S_1^1 &= R_1 \\
S_2^1 + S_2^2 &= 0 \\
S_3^2 &= Q
\end{aligned}
\tag{B.9}
$$

$$
\frac{AE}{\ell}\begin{bmatrix} 1 & -1 & 0 \\ -1 & 2 & -1 \\ 0 & -1 & 1 \end{bmatrix}\begin{Bmatrix} u_1 \\ u_2 \\ u_3 \end{Bmatrix} = \begin{Bmatrix} R_1 \\ 0 \\ Q \end{Bmatrix} \tag{B.10}
$$

$$
[M] = m_o \begin{bmatrix} \frac{1}{2} & 0 & 0 \\ 0 & 1 & 0 \\ 0 & 0 & \frac{1}{2} \end{bmatrix}, \quad m_o = \rho A \ell = \text{mass of one element} \tag{B.11}
$$

$$
[M]\{\ddot{\delta}\} + [K]\{\delta\} = \{R\} \tag{B.12}
$$

Let $Q(t) = QH(t)$.

By following the pattern shown for two elements, the equations for four elements may be written:

$$m_o \begin{bmatrix} \frac{1}{2} & 0 & 0 & 0 & 0 \\ 0 & 1 & 0 & 0 & 0 \\ 0 & 0 & 1 & 0 & 0 \\ 0 & 0 & 0 & 1 & 0 \\ 0 & 0 & 0 & 0 & \frac{1}{2} \end{bmatrix} \begin{Bmatrix} \ddot{u}_1 \\ \ddot{u}_2 \\ \ddot{u}_3 \\ \ddot{u}_4 \\ \ddot{u}_5 \end{Bmatrix} + \frac{AE}{\ell} \begin{bmatrix} 1 & -1 & 0 & 0 & 0 \\ -1 & 2 & -1 & 0 & 0 \\ 0 & -1 & 2 & -1 & 0 \\ 0 & 0 & -1 & 2 & -1 \\ 0 & 0 & 0 & -1 & 1 \end{bmatrix} \begin{Bmatrix} u_1 \\ u_2 \\ u_3 \\ u_4 \\ u_5 \end{Bmatrix}$$

$$= \begin{Bmatrix} R_1 \\ 0 \\ 0 \\ 0 \\ Q(t) \end{Bmatrix} \qquad \text{(B.13)}$$

Divide both sides by $\frac{m_o}{2}$, recall $m_o = \rho A l$, and longitudinal wave speed, $c = \sqrt{E/\rho}$.

$$\ddot{u}_1 + \left(\frac{c}{\ell}\right)^2 (2u_1 - 2u_2) = \frac{2R_1}{m_o}$$

$$2\ddot{u}_2 + \left(\frac{c}{\ell}\right)^2 (-2u_1 + 4u_2 - 2u_3) = 0$$

$$2\ddot{u}_3 + \left(\frac{c}{\ell}\right)^2 (-2u_2 + 4u_4 - 2u_4) = 0 \qquad \text{(B.14)}$$

$$2\ddot{u}_4 + \left(\frac{c}{\ell}\right)^2 (-2u_3 + 4u_4 - 2u_5) = 0$$

$$\ddot{u}_5 + \left(\frac{c}{\ell}\right)^2 (-2u_4 + 2u_5) = \frac{2QH(t)}{m_o}$$

Initially, at $t = 0$, the displacements and velocities of all five nodes are zero. The boundary condition exists such that the left end is fixed, or, the displacement,

velocity and acceleration of node one are zero for all time. This boundary condition means that the Laplace transforms of u_1 and $\ddot{u}_1$, are also zero. The Laplace transforms of the equations with the initial and boundary conditions substituted are:

$$
\begin{aligned}
-\left(\frac{c}{\ell}\right)^2 U_2 &= \frac{L[R_1]}{m_o} \\
s^2 U_2 + \left(\frac{c}{\ell}\right)^2 (2U_2 - U_3) &= 0 \\
s^2 U_3 + \left(\frac{c}{\ell}\right)^2 (-U_2 + 2U_4 - U_4) &= 0 \\
s^2 U_4 + \left(\frac{c}{\ell}\right)^2 (-U_3 + 2U_4 - U_5) &= 0 \\
s^2 U_5 + \left(\frac{c}{\ell}\right)^2 (-2U_4 + 2U_5) &= \frac{2Q}{sm_o}
\end{aligned}
\qquad \text{(B.15)}
$$

where the capital U indicates the Laplace transform of the displacement and s is the Laplace operator.

It is clear from the first equation that U_2 can be expressed as a constant times the transform of R_1. This is substituted for U_2 in the succeeding equations. Then, with that substitution in the second equation, U_3 is expressed in terms of the transform of R_1. The substitutions continue and after substitution and rearrangement the fourth equation expresses U_5 in terms of the transform of R_1. The fifth equation is used to find the transform of R_1 in terms of the transform of the forcing function. The result is separated by partial fractions into recognizable transforms which are the transforms

of sine functions and the transform of the forcing function all multiplied by constants. The inverse of this Laplace expression is the reaction, R_1, as a function of time. At time zero, the four sine terms vanish, and

$$R_1\Big|_{t=+0} = -\frac{Q}{5} . \tag{B.16}$$

Additional elements result in more terms in the series and R_1 at time zero approaches zero.

Consistent Mass Matrix

The mass of the element is considered to be distributed. Its inertia is assumed to act as a body force causing nodal forces, S^b, in combination with the nodal forces, S^e, caused by the stiffness of the element. The virtual work expression must then include the contribution of the mass intertia.

Let $X = \rho\ddot{u}$ = body force.

$$S_i^i u_i + S_j^i u_j = \int_{x_i}^{x_j} \sigma\varepsilon A dx + \int_{x_i}^{x_j} XuA dx \tag{B.17}$$

The displacement function is now variable with position and time.

$$u(x,t) = \alpha_1 + \alpha_2 x(t) \tag{B.18}$$

$$u(x,t) = u_j\left[\frac{x - x_i}{\ell}\right] - u_i\left[\frac{x_j - x}{\ell}\right] \tag{B.19}$$

$$\ddot{u}(x,t) = \ddot{u}_j \left[\frac{x - x_i}{\ell}\right] - \ddot{u}_i \left[\frac{x_j - x}{\ell}\right] \qquad (B.20)$$

rewriting B.17

$$(S^b + S^e)^i_i u_i + (S^b + S^e)^i_j u_j$$

$$= \int_{x_i}^{x_j} \sigma\varepsilon A dx + \int_{x_i}^{x_j} XuA dx \qquad (B.21)$$

The contribution of the inertia forces may be formed by separating the body force terms.

$$(S^b)^i_i u_i + (S^b)^i_j u_j$$

$$= \frac{1}{\ell} \int_{x_i}^{x_j} XA[u_j(x - x_i) - u_i(x - x_j)]dx \qquad (B.22)$$

Equating coefficient of u_i and u_j ;

$$(S^b)^i_i = \frac{1}{\ell} \int_{x_i}^{x_j} XA(x_j - x)dx$$

$$(S^b)^i_j = \frac{1}{\ell} \int_{x_i}^{x_j} XA(x - x_i)dx \qquad (B.23)$$

Substitution of $X = \rho\ddot{u}$,

$$x_i = (i - 1)\ell,$$

$$x_j = i\ell,$$

rearranging, substituting $Z = \left(\frac{x}{\ell} - i\right)$, and with the corresponding changes in the limits of integration, the nodal forces due to inertia forces may be written;

$$(S^b)^i_i = -m_o \int_{-1}^{0} ((\ddot{u}_j - \ddot{u}_i)Z^2 + \ddot{u}_j Z)dZ$$

$$(S^b)^i_j = -(S^b)^i_i - m_o \int_{-1}^{0} ((\ddot{u}_j - \ddot{u}_i)Z + \ddot{u}_j)dZ \qquad \text{(B.24)}$$

Evaluation of the integrals yields;

$$(S^b)^i_i = m_o\left[\frac{\ddot{u}_j}{6} + \frac{\ddot{u}_i}{3}\right]$$

$$(S^b)^i_j = m_o\left[\frac{\ddot{u}_j}{3} + \frac{\ddot{u}_i}{6}\right] \qquad \text{(B.25)}$$

By writing equilibrium of forces at the nodes of the two element problem, remembering that the nodal forces consist of both inertia and elastic forces, the following set of equations is formulated.

$$m_o \begin{bmatrix} \frac{1}{3} & \frac{1}{6} & 0 \\ \frac{1}{6} & \frac{2}{3} & \frac{1}{6} \\ 0 & \frac{1}{6} & \frac{1}{3} \end{bmatrix} \begin{Bmatrix} \ddot{u}_1 \\ \ddot{u}_2 \\ \ddot{u}_3 \end{Bmatrix}$$

$$+ \frac{AE}{\ell} \begin{bmatrix} 1 & -1 & 0 \\ -1 & 2 & -1 \\ 0 & -1 & 1 \end{bmatrix} \begin{Bmatrix} u_1 \\ u_2 \\ u_3 \end{Bmatrix} = \begin{Bmatrix} R_1 \\ 0 \\ Q \end{Bmatrix} \qquad \text{(B.26)}$$

where the first matrix is the so-called consistent mass matrix and the stiffness matrix is the same as before. $M\ddot{\delta}$ plus $K\delta$ give the nodal forces.

After formulating the four element problem with the consistent mass matrix, the solution of the five resulting equations by Laplace transform follows the same procedure as shown for the four element lumped mass problem. The same initial and boundary conditions are used and the reaction at node one is found by successive substitution. Again, the solution is a step plus sine functions all multiplied by constants. At time zero, only the step acts on node one and the constant coefficient is unity. The reaction at $t = 0(+)$ is:

$$R_1\Big|_{t=+0} = -Q \tag{B.27}$$

Even with additional elements, $R_1 \equiv -Q$ at time zero. Therefore, the consistent mass matrix does not allow propagation of transient phenomenon. The reaction, R_1, is a Fourier sine series in which the first term is a constant since the forcing function is a unit step. It is well known that Fourier series solutions for a step, or any discontinuous function, have a jump at the discontinuity known as Gibbs phenomenon and proportional to the size of the discontinuity (See Biot and von Kármán [9]). Further, the above analyses indicate that the dynamic finite elements solutions are equivalent to Fourier series solutions even though the process is numerical in the computer. Therefore, the oscillations in the finite element solution are

due to too few terms in the series (too few nodes) and Gibbs phenomenon.

Finally, it is easy to see that the equations of motion developed by lumping the mass at the nodes are the same as the one dimensional wave equation. The comparison is obvious when the accelerations in the finite element method are written in finite difference notation. Then the differential equation for one-dimensional waves is written in finite difference notation. The finite element stiffness times displacement terms are already equivalent to the difference notation. However, when the accelerations in the finite element equations for the consistent mass matrix are written in difference form, the result does not correspond to the difference form of the one dimensional wave equation. This qualitative look at the nature of the equations further supports the idea that the consistent mass matrix will not allow propagation.

DO NOT PRINT

APPENDIX C

APPENDIX C

COMPUTER PROGRAM JMMSPALL

Following is a listing of the program used in this research. A sample printout is included, consisting of a typical printout for one time step. In use, the program solves a dynamic axisymmetric problem and prints out stresses and displacements at several times. The sample problem is a plate with a distributed load. There are twenty-four nodes axially and thirty-five nodes radially. Distributed loads are produced by resolving the desired stress to nodal forces.

```
      CALL DATSUB(DT,TDT,NNOD,NFS,NF,NELM,A,DE,NZZ)
      CALL SOLVE(NNOD,DT,NFS,NF,TDT,T,NELM,A,DE,NZZ)
      WRITE(6,801)T
  801 FORMAT(///,30X,' T=',E10.4,'PROGRAM SPALL COMPLETE FOR SPECIFIED
     1TIME OF PROPAGATION')
      STOP
      END
```

```
      SUBROUTINE DATSUB(DT,TDT,NNOD,NFS,NF,NELM,A,DE,NZZ)
      DIMENSION DB(24)
      COMMON B(24),KELM(36),KASY(1680,14),MASS(1680),R(840),Z(840),
     1F(45),D(16),NI(1564),NJ(1564),NM(1564),NADJ(840,7),NZRU(560)
      INTEGER*2 NI,NJ,NM,NADJ,NZRU
      REAL KASY,KELM,MASS
      READ(5,1000)DE,E,PR,RHO
 1000 FORMAT(4E10.4)
      READ(5,1004) NF,NELM,NNOD,NCL,NFC,NZZ,NZR
 1004 FORMAT(7I4)
      CMU=E/(2.*(1.+PR))
      CLMBDA=PR*E/((1.+PR)*(1.-2.*PR))
      VDIL=SQRT((CLMBDA+2.*CMU)*386.4/RHO)
      VSHEAR=SQRT(386.4*CMU/RHO)
      DT=.50*DE/VDIL
      TDT=76*DT
      H=(NCL+1)*DE
      WRITE(6,1001) DT,TDT,DE,H,E,PR,RHO
 1001 FORMAT(1H1,//10X,'TIME INCRLMENT, DT=',E11.5,/,10X,'TOTAL TIME ',
     1'OF PROPAGATION=',E11.5,/,10X,'ELEMENT SIZE=',E11.5,/,10X,
     2'PLATE THICKNESS=',E11.5,/,10X,'YOUNGS MODULUS=',E11.5,/,10X,
     3'POISSONS RATIO=',E11.5,/,10X,'WEIGHT DENSITY=',E11.5)
      WRITE(6,1008)VDIL,VSHEAR
 1008 FORMAT(//10X,'DILITATION WAVE SPEED=',E12.5,'INCHES PER SEC',//,
     110X,'DISTORTIONAL WAVE SPEED=',E12.5,'INCHES PER SEC',///10X,
     2'D MATRIX',/)
      DO 9988 I=1,16
 9988 D(I)=0.0
      D(1)=1.-PR
      D(2)=PR
```

```
      D(3)=PR
      D(5)=PR
      D(6)=1.-PR
      D(7)=PR
      D(9)=PR
      D(10)=PR
      D(11)=1.-PR
      D(16)=.5*(1.-2.*PR)
      DO 1002 I=1,4
 1002 WRITE(6,1003) (D(J),J=I,16,4)
 1003 FORMAT(4F10.4)
      READ(5,1005) (F(I),I=1,NF)
 1005 FORMAT(7E11.5)
      P=F(1)
      PI=3.1416
      NF=24
      NFS=NFC-NF+3
      N=NF-1
      DO 9999 IFF=1,N
 9999 F(IFF)=2.*(NF-IFF)*DE*DE*P*PI
      F(NF)=P*PI*DE*DE*.25
      WRITE(6,1104)NF,NELM,NNOD,NCL,NFC,NZZ,NZR
 1104 FORMAT(//,1X,'   NF NELM NNOD  NCL  NFC  NZZ  NZR',/,1X,7I5)
      WRITE(6,1006) (F(I),I=1,NF)
 1006 FORMAT(//,10X,'FORCES',/,10(2X,E11.5))
      ITOP=NZZ-1
      ISUM=0
      DO 1 I=1,ITOP,2
      IBASE=NFC+2
      INC=2*IBASE
```

```
      ISUM=ISUM+INC
      NZRU(I)=IBASE+ISUM-INC
    1 NZRU(I+1)=NZRU(I)+1
      ISUM=0
      ISTART=NZZ+1
      ITOP=NZR-1
      DO 2 I=ISTART,ITOP,2
      IBASE=1
      ISUM=ISUM+INC
      NZRU(I)=IBASE+ISUM-INC
    2 NZRU(I+1)=NZRU(I)+INC-IBASE
      WRITE(6,1107)(NZRU(I),I=1,NZR)
 1107 FORMAT(//,5X,'NZRU',2(/,1X,24I4))
      IN=0
      CZ=-1.0
    5 CZ=CZ+1.0
      CR=NFC+2.
      ICR=CR
      DO 12 I=1,ICR
      CR=CR-1.0
      IN=IN+1
      R(IN)=CR
   12 Z(IN)=CZ
      CR=-1.0
      CZ=CZ+1.0
      DO 20 I=1,ICR
      CR=CR+1.0
      IN=IN+1
      R(IN)=CR
   20 Z(IN)=CZ
```

```
      IF(CZ-NELM/(2*(NFC+1)))5,25,25
   25 DO 30 N=1,NNOD
      R(N)=R(N)*DL
   30 Z(N)=Z(N)*DL
      J=1
      K=NFC+1
      LL=1
      IT=INC
   32 L=LL
      II=0
      DO 40 I=J,K
      II=II+1
      IM=IT-II+1
      NI(L)=I
      NJ(L)=I+1
      NM(L)=IM
      L=L+NELM/(2*(NFC+1))
      NI(L)=I+1
      NJ(L)=IM-1
      NM(L)=IM
   40 L=L+NELM/(2*(NFC+1))
      IF(J-NNOD+INC-1)41,51,51
   41 J=J+INC
      K=J+NFC
      IT=IT+INC
      LL=LL+2
      GO TO 32
   51 J=INC
      K=J+NFC
      IT=INC+1
```

```
      LL=2
   60 L=LL
      II=0
      DO 70 I=J,K
      II=II+1
      IJ=IT-II-1
      NI(L)=IJ+1
      NJ(L)=IJ
      NM(L)=I+1
      L=L+NELM/(2*(NFC+1))
      NI(L)=IJ
      NJ(L)=I+2
      NM(L)=I+1
   70 L=L+NELM/(2*(NFC+1))
      IF(J-NNOD+INC)71,72,72
   71 J=J+INC
      K=J+NFC
      IT=IT+INC
      LL=LL+2
      GO TO 60
   72 CONTINUE
      DO 91 N=1,NNOD
      DO 91 K=1,7
   91 NADJ(N,K)=0
      IC34=NFC+1
      NCLB=NNOD-NFC-1
      NCLF=NFC+2
      NADJ(1,1)=1
      NADJ(1,2)=2
      NADJ(1,3)=INC
```

```
NADJ(NCLB,1)=NCLB-1
NADJ(NCLB,2)=NCLB
NADJ(NCLB,3)=NCLB+1
NADJ(NNOD,1)=NNOD-INC+1
NADJ(NNOD,2)=NNOD-INC+2
NADJ(NNOD,3)=NNOD-1
NADJ(NNOD,4)=NNOD
NADJ(NCLF,1)=IC34
NADJ(NCLF,2)=NCLF
NADJ(NCLF,3)=NCLF+1
NADJ(NCLF,4)=NCLF+2
NADJ(INC,1)=1
NADJ(INC,2)=2
NADJ(INC,3)=INC-1
NADJ(INC,4)=INC
NADJ(INC,5)=INC+1
NADJ(INC+1,1)=INC-1
NADJ(INC+1,2)=INC
NADJ(INC+1,3)=INC+1
NADJ(INC+1,4)=INC+2
NADJ(INC+1,5)=INC+INC
NADJ(NCLF+1,1)=NCLF
NADJ(NCLF+1,2)=NCLF+1
NADJ(NCLF+1,3)=NCLF+2
NADJ(NCLF+1,4)=INC+IC34
NADJ(NCLF+1,5)=INC+IC34+1
NADJ(3*NCLF,1)=NCLF+1
NADJ(3*NCLF,2)=3*NCLF-1
NADJ(3*NCLF,3)=3*NCLF
NADJ(3*NCLF,4)=3*NCLF+1
```

```
      NADJ(3*NCLF,5)=3*NCLF+2
      KK=1
      N=NFC+3
      NTOP=(NZZ-2)/2-1
   77 DO 79 I=1,NTOP
      DO 78 K=1,5
   78 NADJ(N+INC,K)=NADJ(N,K)+INC
   79 N=N+INC
      KK=KK+1
      IF(KK-2)82,82,83
   82 N=INC
   83 IF(KK-3)77,84,85
   84 N=INC+1
   85 IF(KK-4)77,86,87
   86 N=3*NCLF
      GO TO 77
   87 DO 104 N=2,IC34
      NADJ(N,1)=N-1
      NADJ(N,2)=N
      NADJ(N,3)=N+1
      NADJ(N,4)=INC+1-N
  104 NADJ(N,5)=INC+2-N
      IV=NNOD-NFC
      ITV=NNOD-1
      DO 105 N=IV,ITV
      NADJ(N,1)=NCLB-N
      NADJ(N,2)=IV-N
      NADJ(N,3)=N-1
      NADJ(N,4)=N
  105 NADJ(N,5)=N+1
```

```
      I=IC34+3
      J=INC-1
      K=1
  102 I1=I-3
      II=0
      I7=I+2*IC34-1
  106 DO 110 N=I,J
      NADJ (N,1)=I1-II
      NADJ(N,2)=I1-II+1
      NADJ(N,3)=N-1
      NADJ(N,4)=N
      NADJ(N,5)=N+1
      NADJ(N,6)=I7-II-1
      NADJ(N,7)=I7-II
  110 II=II+1
      IF(K-2)111,130,130
  111 IF(I-NNOD+INC+NFC-1)112,120,120
  112 I=I+INC
      J=I+NFC-1
      GO TO 102
  120 K=2
      I=2
  130 IF(I-NNOD+INC-2)131,140,140
  131 I=I+INC
      J=I+NFC-1
      I1=I-4
      II=0
      I7=I+2*IC34
      GO TO 106
  140 CONTINUE
```

```
      C=E/((1.+PR)*(1.-2.*PR))
      DO 10 I=1,16
   10 D(I)=D(I)*C
      NRANGE=2*NNOD
  100 DO 103 I=1,NRANGE
      MASS(I)=0.0
      DO 103 K=1,14
  103 KASY(I,K)=0.0
      DO 101 I=1,24
  101 DB(I)=0.0
   11 DO 50 L=1,NELM
      CALL BFORM(L,RBAR,A)
      CALL JMPRD(D,B,DB,4,4,6)
      IR=1
      DO 90 K=1,6
      DO 90 J=1,6
      KELM(IR)=0.0
      DO 80 I=1,4
      IA=4*(J-1)+I
      IB=4*(K-1)+I
   80 KELM(IR)=KELM(IR)+B(IA)*DB(IB)
   90 IR=IR+1
      A=-A
      DO 49 I=1,36
   49 KELM(I)=6.28*RBAR*A*KELM(I)
      CALL KFORM(L)
   50 CONTINUE
      CALL MFORM(DT,A,DE,NFC,NNOD,NZZ,NCL,NZR,RHO)
      RETURN
      END
```

```
      SUBROUTINE BFORM(L,RBAR,A)
      COMMON B(24),KELM(36),KASY(1680,14),MASS(1680),R(840),Z(840),
     1F(45),D(16),NI(1564),NJ(1564),NM(1564),NADJ(840,7),NZRU(560)
      INTEGER*2 NI,NJ,NM,NADJ,NZRU
      RBAR=(R(NI(L))+R(NJ(L))+R(NM(L)))/3.0
      ZBAR=(Z(NI(L))+Z(NJ(L))+Z(NM(L)))/3.0
      DO 10 I=1,24
   10 B(I)=0.0
      A=0.5*(R(NJ(L))*Z(NM(L))-R(NM(L))*Z(NJ(L))+R(NM(L))*Z(NI(L))-
     1R(NI(L))*Z(NM(L))+R(NI(L))*Z(NJ(L))-R(NJ(L))*Z(NI(L)))
      B(1)=(Z(NJ(L))-Z(NM(L)))/(2.*A)
      B(4)=(R(NM(L))-R(NJ(L)))/(2.*A)
      B(2)=(R(NJ(L))*Z(NM(L))-R(NM(L))*Z(NJ(L)))/(RBAR*2.*A)
     1+B(1)+B(4)*ZBAR/RBAR
      B(7)=B(4)
      B(8)=B(1)
      B(9)=(Z(NM(L))-Z(NI(L)))/(2.*A)
      B(12)=(R(NI(L))-R(NM(L)))/(2.*A)
      B(10)=(R(NM(L))*Z(NI(L))-R(NI(L))*Z(NM(L)))/(RBAR*2.*A)
     1+B(9)+B(12)*ZBAR/RBAR
      B(15)=B(12)
      B(16)=B(9)
      B(17)=(Z(NI(L))-Z(NJ(L)))/(2.*A)
      B(20)=(R(NJ(L))-R(NI(L)))/(2.*A)
      B(18)=(R(NI(L))*Z(NJ(L))-R(NJ(L))*Z(NI(L)))/(RBAR*2.*A)
     1+B(17)+B(20)*ZBAR/RBAR
      B(23)=B(20)
      B(24)=B(17)
      RETURN
      END
```

```
      SUBROUTINE KFORM(L)
      DIMENSION JORD(3)
      COMMON B(24),KELM(36),KASY(1680,14),MASS(1680),R(840),Z(840),
     1F(45),D(16),NI(1564),NJ(1564),NM(1564),NADJ(840,7),NZRU(560)
      INTEGER*2 NI,NJ,NM,NADJ,NZRU
      REAL KELM,KASY
      N=NI(L)
      IT=1
      ICR=1
      IR=2*N-1
    2 NC=NI(L)
      I=1
    3 DO 5 K=1,7
      IF(NC-NADJ(N,K))990,7,5
    5 CONTINUE
    7 JORD(I)=K
    9 NC=NJ(L)
      I=I+1
      IF(I-2)9,3,10
   10 NC=NM(L)
      IF(I-3)9,3,11
   11 ICC=1
   12 JC=2*JORD(ICC)-1
      KASY(IR,JC)=KASY(IR,JC)+KELM(IT)
      JC=2*JORD(ICC)
      KASY(IR,JC)=KASY(IR,JC)+KELM(IT+6)
      ICC=ICC+1
      IT=IT+12
      IF(ICC-3)12,12,13
   13 ICR=ICR+1
```

```
      IR=IR+1
      IT=ICR
      IF(ICR-3)11,20,29
   20 N=NJ(L)
      IR=2*N-1
   29 IF(ICR-5)2,30,39
   30 N=NM(L)
      IR=2*N-1
   39 IF(ICR-6)2,11,40
  990 WRITE(6,991)N
  991 FORMAT(1H1,///,30X,'PROGRAM SPALL TERMINATED DUE TO INCORRECT ',
     1'NADJ DATA FOR NODE N=',I4)
      STOP
   40 RETURN
      END
```

```
      SUBROUTINE MFORM(DT,A,DE,NFC,NNOD,NZZ,NCL,NZR,RHO)
      COMMON B(24),KELM(36),KASY(1680,14),MASS(1680),R(840),Z(840),
     1F(45),D(16),NI(1564),NJ(1564),NM(1564),NADJ(840,7),NZRU(560)
      INTEGER*2 NI,NJ,NM,NADJ,NZRU
      REAL M,MASS
      NS=NNOD-NFC-3
      K=0
      II=1
      MASS(1)=0.333*6.284*RHO*(R(1)-0.333*DE)*A/386.4
      MASS(2)=MASS(1)
      CF=1.0
      III=NZZ+1
C     FRONT FACE NODES
      DR=2.*DE/9.
      I=2
      J=NFC+1
   58 DO 60 N=I,J
      IRM=2*N-1
      M=CF*6.284*RHO*(R(N)+DR)*A/386.4
      MASS(IRM)=M
      MASS(IRM+1)=M
   60 CONTINUE
C     INTERIOR NODES
   61 I=N+3
      CF=2.0
      J=I+NFC-1
      DR=0.0
      IF(J-NS)58,58,62
C     BACK FACE NODES
   62 DR=-2.*DE/9.0
```

```
      CF=1.0
      IF(I-NNOD)58,63,63
   63 K=1
C     CL NODES
      DR=4.*DE/9.0
      CF=1.0
      II=II+1
      N=NZRU(II)
      IF(II-(NCL+1))59,59,64
   64 K=2
C     BOUNDARY NODES
      CF=1.0
      DR=-4.*DE/9.0
      III=III+1
      N=NZRU(III)
      IF(III-NZR)59,65,65
   65 K=K+1
      IF(K-3)65,66,67
C     NODE ON FRONT FACE, CL
   66 CF=2./3.
      DR=DE/2.0
      N=NFC+2
      GO TO 59
C     NODE ON BACK FACE, CL
   67 CF=1./3.
      DR=DE/3.
      N=NNOD-NFC-1
      IF(K-4)66,59,68
   59 IRM=2*N-1
      M=CF*6.284*RHO*(R(N)+DR)*A/386.4
```

```
      MASS(IRM)=M
      MASS(IRM+1)=M
      IF(K-1)63,63,601
  601 IF(K-2)64,64,65
   68 RETURN
      END
```

```
      SUBROUTINE SOLVE(NNOD,DT,NFS,NF,TDT,T,NELM,A,DE,NZZ)
      DIMENSION UELM(6),STRAIN(4),STRESS(4),U(1680),UM1(1680),UP1(1680),
     1ANS(2,25)
      COMMON B(24),KELM(36),KASY(1680,14),MASS(1680),R(840),Z(840),
     1F(45),D(16),NI(1564),NJ(1564),NM(1564),NADJ(840,7),NZRU(560)
      INTEGER*2 NI,NJ,NM,NADJ,NZRU
      REAL MASS,KASY
      IFF=0
      ANS(2,1)=0.0
      PI=3.14159
      NCL=NZZ-2
      TTF=45*DT
      TPR=76*DT
      T=0.0
      NN=NNOD*2
      DO 200 I=1,NN
      UM1(I)=0.0
      U(I)=0.0
  200 UP1(I)=0.0
      NN=NNOD-1
      NNN=2*NN
      DO 250 N=1,NN
      UP1(1)=0.0
      IF(N-NFS)205,201,201
  201 IFF=IFF+1
      IF(IFF-NF)202,202,205
  202 FORCE=F(IFF)*0.01
      WFORCE=FORCE
      GO TO 206
  205 FORCE=0.0
```

```
206 IRR=2*N-1
    IRZ=IRR+1
    SUMKUR=0.0
    SUMKUZ=0.0
    DO 210 J=1,7
    IF(NADJ(N,J))249,249,207
207 IC=2*J
    IUR=2*NADJ(N,J)-1
    IUZ=IUR+1
    SUMKUR=SUMKUR+KASY(IRR,IC-1)*U(IUR)+KASY(IRR,IC)*U(IUZ)
210 SUMKUZ=SUMKUZ+KASY(IRZ,IC-1)*U(IUR)+KASY(IRZ,IC)*U(IUZ)
249 UP1(IRR)=U(IRR)-DT*DT*SUMKUR/(2.0*MASS(IRR))
250 UP1(IRZ)=U(IRZ)+DT*DT*(FORCE-SUMKUZ)/(2.0*MASS(IRZ))
    NSTEP=2*(NCL+1)
259 CONTINUE
    U(1)=0.0
    NSTART=1
    NTOP=NELM-2*(NCL+1)+1
    IFF=0
    DO 260 I=2,NNN
    UM1(I)=U(I)
260 U(I)=UP1(I)
    WRITE(6,262)T,WFORCE
262 FORMAT(/,25X,'T=',E12.5,5X,'FORCE=',E12.5)
    DO 263 NR=1,NZZ
    IU=2*NZRU(NR)-1
263 U(IU)=0.0
    IF(T.LT.TPR) GO TO 703
    WRITE(6,220)T
220 FORMAT(1H1,40X,'          STRESS FIELD BY AVERAGING ADJACENT ',
```

```
     1'ELEMENTS',//,59X,'R&Z  COMPONENTS',10X,'T=',E12.5,//,3X,'RCENT')
C      BY ELEMENT, COMPUTE STRAIN & STRESS
       DO 722 N=NSTART,NTOP,NSTEP
       LRT=N+NCL
       ICOUNT=1
       DO 702 LL=N,LRT
       SUMSIG=0.0
       SUMEP=0.0
       L=LL-NCL-1
       DO 699 K=1,2
       L=L+NCL+1
       UELM(1)=U(2*NI(L)-1)
       UELM(2)=U(2*NI(L))
       UELM(3)=U(2*NJ(L)-1)
       UELM(4)=U(2*NJ(L))
       UELM(5)=U(2*NM(L)-1)
       UELM(6)=U(2*NM(L))
       SUMU=0.0
       DO 500 I=1,6
   500 SUMU=SUMU+UELM(I)
       IF(SUMU)501,490,501
   490 DO 492 I=1,4
       STRESS(I)=0.0
   492 STRAIN(I)=0.0
       GO TO 698
   501 CALL BFORM(L,RBAR,A)
       CALL JMPRD(B,UELM,STRAIN,4,6,1)
       CALL JMPRD(D,STRAIN,STRESS,4,4,1)
   698 SUMSIG=SUMSIG+STRESS(1)
       SUMEP=SUMEP+STRESS(3)
```

```
699 CONTINUE
    ICOUNT=ICOUNT+1
    ANS(1,ICOUNT)=.5*SUMSIG*.001
    ANS(2,ICOUNT)=.5*SUMEP*.001
702 CONTINUE
    ANS(1,1)=(R(NJ(L))+R(NM(L)))*.5
    WRITE(6,225)(ANS(1,J),J=1,NZZ)
    WRITE(6,224)(ANS(2,J),J=2,NZZ)
224 FORMAT(10X,23F5.2)
225 FORMAT(/,1X,F5.2,4X,24F5.2)
226 FORMAT(10X,24F5.1)
722 CONTINUE
    ANS(2,1)=DE*0.5+Z(NJ(N))
    DO 723 KZ=1,NZZ
723 ANS(2,KZ+1)=ANS(2,KZ)+DE
    KZ=KZ-1
    WRITE(6,227)(ANS(2,J),J=1,KZ)
227 FORMAT(//,4X,'ZCENT=',24F5.2)
    WRITE(6,230)
230 FORMAT(///,20X,'EACH BLOCK IS   R STRESS IN KSI',
   1/,36X,'Z STRESS IN KSI')
    WRITE(6,228)T
228 FORMAT(1H1,//,57X,'NODAL DISPLACEMENTS',10X,'T=',E12.5,//,2X,
   1'RCENT')
    DO 726 LL=NSTART,NTOP,NSTEP
    ANS(1,1)=R(NI(LL))
    ANS(1,2)=U(2*NI(LL)-1)*1000000.
    ANS(2,2)=U(2*NI(LL))*1000000.
    L=LL-1
    NTOPP=NZZ+1
```

```
      DO 725 N=3,NTOPP
      L=L+1
      ANS(1,N)=U(2*NM(L)-1)*1000000.
  725 ANS(2,N)=U(2*NM(L))*1000000.
      WRITE(6,229)(ANS(1,J),J=1,NTOPP)
  726 WRITE(6,226)(ANS(2,J),J=2,NTOPP)
  229 FORMAT(/,1X,F5.2,4X,24F5.1)
      LL=LL+NCL+1
      ANS(1,1)=R(NI(LL))
      ANS(1,2)=U(2*NI(LL)-1)*1000000.
      ANS(2,2)=U(2*NI(LL))*1000000.
      L=LL-1
      DO 727 N=3,NTOPP
      L=L+1
      ANS(1,N)=U(2*NJ(L)-1)*1000000.
  727 ANS(2,N)=U(2*NJ(L))*1000000.
      WRITE(6,229)(ANS(1,J),J=1,NTOPP)
      WRITE(6,226)(ANS(2,J),J=2,NTOPP)
      ANS(2,1)=Z(NJ(NSTART))
      DO 728 KZ=1,NZZ
  728 ANS(2,KZ+1)=ANS(2,KZ)+DE
      WRITE(6,227)(ANS(2,J),J=1,NZZ)
      WRITE(6,231)
  231 FORMAT(///,20X,'EACH BLOCK IS   RADIAL DISPLACEMENT IN MICRO',
     1'INCHES',/,37X,'  Z   DISPLACEMENT IN MICROINCHES')
      TPR=TPR+2.*DT
  703 IF(T-TDT)271,460,460
  271 T=T+DT
      DO 350 N=1,NN
      U(1)=0.0
```

```
      UP1(1)=0.0
      IF(N-NFS)305,301,301
  301 IFF=IFF+1
      IF(IFF-NF)302,302,305
  302 IF(T-TTF)303,305,305
  303 FORCE=F(IFF)*(1.+SIN(2.*PI*T/TTF-PI/2.))*0.5
      WFORCE=FORCE
      GO TO 306
  305 FORCE=0.0
  306 IRR=2*N-1
      IRZ=IRR+1
      SUMKUR=0.0
      SUMKUZ=0.0
      DO 310 J=1,7
      IF(NADJ(N,J))349,349,307
  307 IC=2*J
      IUR=2*NADJ(N,J)-1
      IUZ=IUR+1
      SUMKUR=SUMKUR+KASY(IRR,IC-1)*U(IUR)+KASY(IRR,IC)*U(IUZ)
  310 SUMKUZ=SUMKUZ+KASY(IRZ,IC-1)*U(IUR)+KASY(IRZ,IC)*U(IUZ)
  349 UP1(IRR)=2*U(IRR)-UM1(IRR)-DT*DT*SUMKUR/MASS(IRR)
  350 UP1(IRZ)=2*U(IRZ)-UM1(IRZ)+DT*DT*(FORCE-SUMKUZ)/MASS(IRZ)
      GO TO 259
  460 RETURN
      END
```

```
      SUBROUTINE JMPRD(A,B,RR,N,MM,L)
      DIMENSION A(1),B(1),RR(1)
      IR=1
      DO 90 K=1,L
      DO 90 J=1,N
      RR(IR)=0.0
      DO 80 I=1,MM
      IA=N*(I-1)+J
      IB=MM*(K-1)+I
   80 RR(IR)=RR(IR)+A(IA)*B(IB)
   90 IR=IR+1
      RETURN
      END
```

TIME INCREMENT, DT=0.83639E-07
TOTAL TIME OF PROPAGATION=0.64402E-05
ELEMENT SIZE=0.40000E-01
PLATE THICKNESS=0.92000E 00
YOUNGS MODULUS=0.10700E 08
POISSONS RATIO=0.31250E 00
WEIGHT DENSITY=0.10100E 00

DILITATION WAVE SPEED= 0.23912E 06INCHES PER SEC

DISTORTIONAL WAVE SPEED= 0.12486E 06INCHES PER SEC

D MATRIX

0.6875	0.3125	0.3125	0.0
0.3125	0.6875	0.3125	0.0
0.3125	0.3125	0.6875	0.0
0.0	0.0	0.0	0.1875

NF	NELM	NNOD	NCL	NFC	NZZ	NZR
24	1564	840	22	33	24	48

FORCES

0.23122E 03 0.22117E 03 0.21112E 03 0.20106E 03 0.19101E 03 0.18096E 03 0.17090E 03 0.16085E 03 0.15080E 03 0.14074E 03
0.13069E 03 0.12064E 03 0.11058E 03 0.10053E 03 0.90478E 02 0.80425E 02 0.70372E 02 0.60319E 02 0.50266E 02 0.40212E 02
0.30159E 02 0.20106E 02 0.10053E 02 0.12566E 01

NZRU

35	36	105	106	175	176	245	246	315	316	385	386	455	456	525	526	595	596	665	666	735	736	805	806
1	70	71	140	141	210	211	280	281	350	351	420	421	490	491	560	561	630	631	700	701	770	771	840

T= 0.0 FORCE= 0.12566E-01

T= 0.83639E-07 FORCE= 0.61150E-02

T= 0.16728E-06 FORCE= 0.24340E-01

T= 0.25092E-06 FORCE= 0.54321E-01

STRESS FIELD BY AVERAGING ADJACENT ELEMENTS

RCZ COMPONENTS T= 0.1A523UE-05

RCENT

1.34 0.17 0.02-0.01-0.01-0.01-0.01-0.01-0.00 0.01 0.02 0.03 0.04 0.04 0.04 0.04 0.03 0.02 0.01 0.00-0.01-0.01-0.98
-0.03-0.07-0.09-0.08-0.07-0.05-0.02 0.02 0.07 0.12 0.17 0.22 0.25 0.27 0.27 0.23 0.16 0.07-0.04-0.16-0.31-0.43-0.53

1.30 0.13 0.03-0.01-0.03-0.03-0.02-0.01 0.02 0.04 0.06 0.09 0.10 0.12 0.12 0.11 0.10 0.08 0.05 0.02-0.01-0.05-0.09-0.69
0.01-0.01-0.02-0.02-0.02-0.01 0.01 0.02 0.04 0.07 0.10 0.14 0.17 0.20 0.22 0.22 0.20 0.17 0.11 0.02-0.07-0.18-0.29-0.38

1.26 0.09 0.02-0.02-0.03-0.03-0.02 0.00 0.03 0.07 0.11 0.14 0.16 0.17 0.18 0.17 0.16 0.11 0.08 0.03-0.04-0.10-0.29-0.30
0.02 0.02 0.02 0.02 0.02 0.02 0.02 0.02 0.02 0.03 0.05 0.08 0.12 0.16 0.19 0.20 0.18 0.15 0.09 0.03-0.04-0.12-0.20-0.26

1.22 0.06 0.01-0.02-0.04-0.03-0.01 0.02 0.06 0.10 0.15 0.18 0.21 0.22 0.22 0.21 0.18 0.15 0.11 0.05-0.03-0.13-0.23-0.30
0.02 0.03 0.04 0.04 0.03 0.03 0.02 0.01-0.00-0.00 0.01 0.04 0.09 0.13 0.18 0.20 0.21 0.19 0.16 0.11 0.04-0.04-0.16-0.23

1.18 0.02-0.01-0.02-0.03-0.02 0.01 0.04 0.09 0.13 0.18 0.22 0.25 0.26 0.26 0.24 0.22 0.18 0.14 0.08-0.00-0.09-0.19-0.26
0.02 0.03 0.03 0.04 0.03 0.02 0.01-0.01-0.02-0.02-0.01 0.02 0.07 0.13 0.19 0.23 0.24 0.24 0.22 0.18 0.12 0.05-0.02-0.09

1.14 -0.03-0.02-0.02-0.01-0.01 0.04 0.07 0.12 0.16 0.21 0.25 0.28 0.29 0.28 0.27 0.24 0.21 0.17 0.11 0.04-0.03-0.13-0.23
0.01 0.02 0.02 0.02 0.02 0.00-0.01-0.03-0.04-0.04-0.02 0.02 0.08 0.15 0.21 0.26 0.29 0.29 0.28 0.24 0.19 0.12 0.04-0.04

1.10 -0.06-0.03-0.01 0.01 0.04 0.07 0.11 0.15 0.19 0.23 0.27 0.29 0.30 0.30 0.28 0.26 0.23 0.19 0.14 0.07-0.00-0.09-0.18
0.00 0.00 0.01 0.00-0.00-0.02-0.03-0.04-0.05-0.04-0.01 0.04 0.10 0.17 0.24 0.30 0.33 0.34 0.33 0.29 0.23 0.15 0.05

1.06 -0.06-0.02 0.01 0.03 0.06 0.10 0.13 0.17 0.21 0.24 0.27 0.29 0.30 0.30 0.29 0.27 0.25 0.21 0.17 0.11 0.04-0.04-0.12
-0.01-0.01-0.01-0.01-0.01-0.02-0.03-0.04-0.05-0.05-0.03 0.01 0.07 0.14 0.21 0.28 0.34 0.38 0.39 0.38 0.33 0.26 0.17 0.06

1.02 -0.05-0.00 0.03 0.06 0.08 0.12 0.15 0.18 0.21 0.24 0.27 0.29 0.30 0.30 0.29 0.28 0.26 0.24 0.20 0.16 0.11 0.04-0.05
-0.01-0.01-0.02-0.02-0.02-0.03-0.04-0.04-0.05-0.04-0.01 0.04 0.11 0.18 0.25 0.32 0.38 0.42 0.44 0.42 0.37 0.29 0.18 0.06

0.98 -0.01 0.02 0.05 0.07 0.10 0.13 0.15 0.18 0.20 0.23 0.25 0.27 0.28 0.29 0.29 0.28 0.28 0.26 0.23 0.18 0.13 0.06-0.01
-0.01-0.01-0.01-0.01-0.02-0.03-0.03-0.04-0.03-0.01 0.02 0.08 0.15 0.23 0.30 0.36 0.42 0.46 0.48 0.45 0.40 0.31 0.20 0.07

0.94 0.03 0.04 0.06 0.08 0.11 0.13 0.15 0.17 0.19 0.21 0.23 0.25 0.27 0.28 0.29 0.29 0.29 0.28 0.26 0.22 0.17 0.11 0.04
-0.01-0.00-0.01-0.01-0.01-0.02-0.02-0.02-0.01 0.02 0.06 0.12 0.19 0.26 0.34 0.40 0.46 0.49 0.51 0.48 0.42 0.33 0.23 0.07

0.90 0.06 0.07 0.07 0.09 0.10 0.12 0.14 0.15 0.17 0.19 0.21 0.23 0.25 0.27 0.28 0.30 0.31 0.31 0.29 0.25 0.21 0.14 0.08
-0.00 0.00-0.00-0.00-0.00-0.00 0.00 0.02 0.04 0.09 0.16 0.24 0.32 0.38 0.43 0.49 0.52 0.53 0.51 0.44 0.35 0.22 0.08

0.86 0.09 0.08 0.08 0.09 0.10 0.11 0.12 0.13 0.15 0.16 0.18 0.21 0.24 0.26 0.28 0.31 0.33 0.33 0.32 0.28 0.24 0.18 0.11
0.00 0.01 0.01 0.01 0.01 0.01 0.02 0.04 0.07 0.12 0.19 0.27 0.35 0.41 0.46 0.51 0.54 0.56 0.53 0.46 0.37 0.23 0.08

0.82 0.10 0.09 0.08 0.09 0.09 0.10 0.11 0.11 0.13 0.14 0.16 0.19 0.22 0.25 0.29 0.32 0.34 0.36 0.34 0.31 0.27 0.21 0.15
0.00 0.01 0.01 0.02 0.02 0.03 0.04 0.06 0.10 0.15 0.22 0.31 0.38 0.44 0.48 0.53 0.57 0.58 0.55 0.46 0.38 0.26 0.06

0.78 0.10 0.09 0.08 0.08 0.08 0.08 0.09 0.09 0.10 0.11 0.13 0.17 0.22 0.25 0.29 0.33 0.37 0.38 0.37 0.34 0.29 0.24 0.18
0.00 0.02 0.02 0.03 0.03 0.04 0.05 0.07 0.12 0.18 0.25 0.33 0.41 0.46 0.50 0.55 0.58 0.60 0.57 0.51 0.42 0.26 0.09

0.74 0.10 0.09 0.07 0.07 0.06 0.06 0.07 0.07 0.07 0.09 0.11 0.16 0.21 0.26 0.31 0.35 0.39 0.41 0.43 0.37 0.33 0.27 0.20
0.00 0.02 0.03 0.04 0.04 0.05 0.07 0.09 0.14 0.20 0.27 0.35 0.43 0.47 0.51 0.56 0.60 0.62 0.60 0.53 0.42 0.27 0.09

0.70 0.10 0.08 0.06 0.05 0.04 0.04 0.04 0.04 0.04 0.06 0.10 0.15 0.21 0.27 0.32 0.38 0.42 0.44 0.43 0.40 0.35 0.29 0.23
0.00 0.02 0.03 0.05 0.05 0.06 0.08 0.11 0.15 0.21 0.28 0.36 0.43 0.48 0.52 0.57 0.60 0.65 0.62 0.55 0.44 0.28 0.09

0.66 0.09 0.06 0.04 0.03 0.02 0.01 0.01 0.01 0.01 0.04 0.09 0.15 0.23 0.29 0.35 0.41 0.45 0.46 0.45 0.42 0.38 0.32 0.25
0.01 0.03 0.04 0.05 0.06 0.07 0.09 0.12 0.16 0.22 0.28 0.36 0.43 0.48 0.53 0.58 0.64 0.68 0.65 0.58 0.46 0.29 0.10

0.62 0.08 0.04 0.01 0.00-0.01-0.02-0.02-0.02-0.02-0.00 0.03 0.09 0.17 0.25 0.32 0.38 0.44 0.47 0.49 0.49 0.45 0.40 0.34 0.27
0.01 0.03 0.04 0.06 0.06 0.08 0.10 0.12 0.16 0.21 0.27 0.35 0.42 0.47 0.53 0.60 0.67 0.71 0.69 0.61 0.49 0.31 0.10

0.58 0.04 0.01-0.02-0.03-0.04-0.04-0.05-0.05-0.04-0.01 0.04 0.10 0.19 0.28 0.35 0.41 0.47 0.50 0.52 0.52 0.47 0.43 0.36 0.29
0.01 0.04 0.04 0.06 0.07 0.08 0.09 0.11 0.14 0.19 0.25 0.33 0.42 0.47 0.53 0.61 0.70 0.75 0.73 0.65 0.51 0.33 0.11

0.54 -0.01-0.04-0.06-0.06-0.07-0.06-0.05-0.04 0.00 0.06 0.13 0.22 0.32 0.39 0.45 0.51 0.53 0.54 0.53 0.49 0.45 0.38 0.31
0.02 0.05 0.04 0.05 0.06 0.07 0.08 0.09 0.11 0.15 0.21 0.30 0.39 0.46 0.54 0.64 0.73 0.79 0.77 0.68 0.54 0.34 0.11

0.50 -0.09-0.10-0.09-0.09-0.08-0.06-0.05-0.02 0.03 0.09 0.17 0.27 0.36 0.43 0.49 0.53 0.56 0.57 0.55 0.51 0.47 0.40 0.32
0.01 0.02 0.02 0.03 0.04 0.04 0.05 0.05 0.07 0.11 0.18 0.27 0.37 0.46 0.56 0.67 0.77 0.83 0.81 0.72 0.57 0.36 0.12

0.46 -0.18-0.15-0.12-0.10-0.08-0.05-0.02 0.01 0.07 0.13 0.22 0.31 0.40 0.47 0.52 0.56 0.59 0.59 0.57 0.53 0.48 0.41 0.33
0.00 0.00 0.00 0.01 0.00 0.01 0.00 0.01 0.02 0.07 0.14 0.24 0.36 0.47 0.59 0.71 0.82 0.88 0.85 0.76 0.60 0.38 0.13

0.42 -0.26-0.18-0.14-0.09-0.06-0.03 0.01 0.05 0.11 0.18 0.26 0.36 0.44 0.51 0.55 0.59 0.61 0.62 0.59 0.55 0.50 0.42 0.33
-0.01-0.02-0.03-0.02-0.03-0.04-0.04-0.04-0.02 0.03 0.11 0.23 0.38 0.49 0.62 0.76 0.87 0.92 0.90 0.80 0.63 0.40 0.13

0.38 -0.31-0.20-0.14-0.08-0.04 0.00 0.04 0.09 0.15 0.22 0.31 0.39 0.48 0.54 0.58 0.62 0.64 0.62 0.57 0.51 0.43 0.34
-0.02-0.04-0.05-0.05-0.06-0.07-0.08-0.08-0.08-0.10 0.09 0.23 0.39 0.53 0.67 0.81 0.92 0.97 0.94 0.84 0.66 0.42 0.14

0.34 -0.31-0.23-0.12-0.06-0.02 0.03 0.08 0.13 0.19 0.26 0.34 0.42 0.50 0.56 0.61 0.65 0.67 0.67 0.64 0.59 0.52 0.44 0.34
-0.03-0.05-0.06-0.07-0.09-0.10-0.11-0.12-0.08-0.01 0.10 0.25 0.42 0.57 0.72 0.86 0.97 1.02 0.99 0.88 0.69 0.44 0.15

0.30 -0.27-0.17-0.10-0.04 0.01 0.06 0.11 0.16 0.22 0.28 0.36 0.44 0.52 0.56 0.64 0.68 0.70 0.70 0.67 0.61 0.54 0.44 0.33
-0.03-0.05-0.07-0.08-0.10-0.11-0.12-0.11-0.08-0.02 0.12 0.28 0.46 0.62 0.77 0.91 1.02 1.07 1.03 0.94 0.72 0.46 0.15

0.26 -0.19-0.12-0.07-0.02 0.03 0.06 0.13 0.18 0.24 0.30 0.37 0.45 0.54 0.61 0.66 0.71 0.73 0.73 0.69 0.63 0.55 0.45 0.33
-0.03-0.04-0.07-0.08-0.10-0.11-0.12-0.10-0.06 0.03 0.15 0.32 0.52 0.67 0.82 0.96 1.06 1.11 1.07 0.95 0.75 0.48 0.16

0.22 -0.10-0.07-0.03 0.01 0.06 0.10 0.15 0.19 0.25 0.31 0.38 0.47 0.56 0.63 0.69 0.74 0.77 0.76 0.72 0.65 0.56 0.45 0.33
-0.02-0.03-0.06-0.08-0.10-0.12-0.10-0.08-0.03 0.06 0.19 0.36 0.54 0.71 0.86 1.00 1.10 1.15 1.11 0.98 0.76 0.50 0.16

0.18 -0.03-0.02 0.01 0.04 0.08 0.12 0.16 0.20 0.25 0.32 0.39 0.48 0.57 0.65 0.71 0.76 0.79 0.79 0.74 0.67 0.57 0.44 0.33
-0.01-0.02-0.05-0.07-0.09-0.09-0.08-0.06 0.00 0.09 0.22 0.39 0.58 0.74 0.90 1.04 1.14 1.19 1.14 1.01 0.81 0.51 0.17

0.14 0.03 0.03 0.04 0.07 0.10 0.14 0.17 0.21 0.26 0.32 0.40 0.49 0.58 0.66 0.73 0.79 0.82 0.81 0.76 0.68 0.58 0.46 0.33
-0.01-0.02-0.05-0.07-0.08-0.08-0.07-0.04 0.03 0.12 0.25 0.42 0.60 0.77 0.93 1.07 1.17 1.22 1.17 1.04 0.83 0.53 0.17

0.10 0.07 0.06 0.07 0.10 0.12 0.15 0.18 0.22 0.27 0.33 0.41 0.50 0.60 0.68 0.75 0.81 0.84 0.83 0.78 0.69 0.57 0.42 0.26
-0.01-0.03-0.05-0.07-0.08-0.07-0.06-0.02 0.04 0.14 0.27 0.44 0.62 0.79 0.95 1.10 1.20 1.24 1.20 1.06 0.84 0.54 0.17

0.06 0.09 0.10 0.11 0.14 0.16 0.19 0.23 0.28 0.34 0.42 0.51 0.61 0.69 0.76 0.82 0.85 0.84 0.79 0.70 0.59 0.47 0.34
-0.01-0.03-0.06-0.07-0.08-0.07-0.05-0.01 0.06 0.15 0.28 0.45 0.63 0.81 0.97 1.12 1.23 1.27 1.22 1.08 0.86 0.56 0.18

0.02 0.10 0.10 0.11 0.12 0.14 0.17 0.19 0.23 0.28 0.34 0.42 0.52 0.61 0.70 0.76 0.82 0.86 0.85 0.80 0.71 0.59 0.46 0.33
-0.01-0.04-0.06-0.08-0.08-0.07-0.04-0.00 0.06 0.14 0.28 0.46 0.64 0.82 0.98 1.13 1.26 1.29 1.24 1.11 0.88 0.56 0.13

ZCENT= 0.02 0.06 0.10 0.14 0.18 0.22 0.26 0.30 0.34 0.38 0.42 0.46 0.50 0.54 0.58 0.62 0.66 0.70 0.74 0.78 0.82 0.86 0.90

EACH BLOCK IS R STRESS IN KSI
Z STRESS IN KSI

NODAL DISPLACEMENTS T= 0.652286E-05

RCENT																						
1.36	0.0	-0.8	-0.3	0.6	1.8	3.3	5.1	7.0	9.0	10.8	12.4	13.6	14.3	14.4	14.1	13.2	12.0	10.6	9.2	8.0	6.9	6.	4.7	3.0
	6.0	5.4	4.9	4.5	4.1	3.7	3.5	3.3	3.4	3.6	4.0	4.5	5.3	6.2	7.1	8.0	8.7	9.1	9.2	8.9	8.1	6.	4.6	0.0
1.32	-1.1	-1.0	-0.5	0.5	1.7	3.3	5.2	7.1	9.1	11.0	12.6	13.9	14.6	14.8	14.5	13.6	12.3	10.8	9.3	7.9	6.7	5.8	4.6	4.2
	5.9	5.7	5.6	5.5	5.4	5.2	5.2	5.1	5.1	5.1	5.2	5.5	5.8	6.2	6.7	7.3	7.8	8.1	8.3	8.1	7.7	6.	5.7	6.3
1.28	-1.7	-1.2	-0.5	0.5	1.8	3.4	5.3	7.2	9.2	11.0	12.6	13.9	14.7	14.9	14.6	13.7	12.5	10.9	9.3	7.9	6.7	5.8	5.4	6.1
	6.5	6.4	6.5	6.5	6.6	6.6	6.6	6.6	6.5	6.4	6.3	6.3	6.4	6.6	7.0	7.5	7.6	7.6	7.9	7.	7.6	7.8	8.4	
1.24	-2.2	-1.3	-0.4	0.7	2.0	3.6	5.4	7.3	9.1	10.9	12.4	13.6	14.4	14.6	14.4	13.6	12.4	11.0	9.4	8.1	7.0	6.5	6.7	7.5
	7.5	7.4	7.5	7.6	7.8	7.9	8.0	8.0	7.9	7.7	7.4	7.1	6.9	6.7	6.6	6.9	7.2	7.5	7.9	8.1	8.4	8.7	9.2	9.7
1.20	-2.5	-1.4	-0.3	0.8	2.2	3.8	5.5	7.2	8.9	10.6	11.9	13.1	13.9	14.2	14.2	13.8	12.8	11.0	9.5	8.3	7.5	7.	7.7	8.6
	8.6	8.7	8.8	8.9	9.1	9.2	9.3	9.2	9.0	8.7	8.3	7.8	7.4	7.2	7.1	7.2	7.4	7.8	8.3	8.7	9.2	9.7		10.6
1.16	-2.6	-1.4	-0.2	1.0	2.4	3.9	5.5	7.1	8.6	10.1	11.4	12.4	13.2	13.6	13.6	13.1	12.1	10.9	9.6	8.6	8.3		8.7	9.8
	10.0	10.1	10.2	10.3	10.5	10.5	10.5	10.3	10.0	9.6	9.0	8.5	8.0	7.7	7.6	7.7	8.0	8.5	9.0	9.6				
1.12	-2.5	-1.3	-0.1	1.1	2.4	3.9	5.4	6.8	8.2	9.5	10.6	11.7	12.5	12.9	13.0	12.7	11.9	10.9	9.7	8.8				
	11.4	11.5	11.6	11.7	11.7	11.7	11.5	11.2	10.8	10.3	9.7	9.1	8.6	8.3	8.2	8.4	8.8	9.4						
1.08	-2.3	-1.2	-0.1	1.1	2.4	3.7	5.1	6.4	7.6	8.8	9.9	10.8	11.7	12.3	12.5	12.3	11.7	10.8	9.7	9.0				
	12.7	12.8	12.9	12.9	12.8	12.6	12.4	12.0	11.5	10.9	10.3	9.7	9.3	9.1	9.1	9.4	9.9							
1.04	-2.0	-1.1	-0.1	1.0	2.2	3.5	4.7	5.9	7.0	8.1	9.1	10.1	11.0	11.7	12.1	12.3	11.5	10.7						
	13.7	13.8	13.8	13.7	13.6	13.3	13.0	12.6	12.0	11.5	10.9	10.5	10.2	10.1	10.3	10.7								
1.00	-1.8	-1.0	-0.1	0.9	2.0	3.1	4.3	5.4	6.4	7.4	8.3	9.3	10.3	11.1	11.6	11.7	11.4	10.6						
	14.4	14.5	14.4	14.3	14.1	13.9	13.5	13.1	12.6	12.1	11.6	11.3	11.2	11.3	11.6									
0.96	-1.7	-1.1	-0.3	0.7	1.7	2.7	3.8	4.8	5.8	6.7	7.7	8.7	9.6	10.7	11.3	11.5	11.2							
	15.0	14.9	14.9	14.7	14.5	14.3	13.9	13.6	13.1	12.8	12.5	12.3	12.4	12.7										
0.92	-1.8	-1.2	-0.5	0.4	1.4	2.3	3.3	4.3	5.2	6.2	7.2	8.3	9.4	10.4	11.1	11.4	11.1							
	15.4	15.3	15.2	15.1	15.0	14.7	14.5	14.2	13.8	13.6	13.4	13.5	13.7											
0.88	-2.1	-1.4	-0.7	0.2	1.1	2.0	2.9	3.9	4.8	5.7	6.8	8.0	9.2	10.2	11.0	11.3								
	15.9	15.8	15.7	15.6	15.5	15.3	15.1	14.9	14.7	14.6	14.6	14.8	15.2											
0.84	-2.4	-1.7	-1.0	-0.1	0.8	1.7	2.6	3.5	4.5	5.4	6.6	7.8	9.0	10.1	10.9	11.2								
	16.4	16.3	16.2	16.2	16.1	16.0	15.9	15.7	15.7	15.7	15.8	16.1												
0.80	-2.8	-2.1	-1.2	-0.4	0.5	1.4	2.4	3.3	4.2	5.3	6.4	7.7	9.0											
	17.1	17.0	16.9	16.9	16.8	16.8	16.8	16.7	16.7	16.8														
0.76	-3.2	-2.4	-1.5	-0.6	0.3	1.2	2.2	3.1	4.1	5.2														
	17.9	17.8	17.8	17.7	17.7	17.8	17.8	17.8	17.9															
0.72	-3.7	-2.7	-1.8	-0.8	0.1	1.1	2.1	3.1	4.1	5.3	6.6	8.0	9.2											
	18.8	18.7	18.7	18.7	18.8	18.8	18.9	19.0	19.2	19.5	20.0													
0.68	-4.1	-3.1	-2.0	-1.0	0.1	1.1	2.1	3.1	4.3	5.5	6.8													
	19.8	19.8	19.8	19.8	19.9	20.1	20.2	20.4	20.7	21.1														
0.64	-4.6	-3.3	-2.2	-1.0	0.1	1.1	2.2	3.3	4.5	5.8	7.2													
	21.0	20.9	21.0	21.1	21.3	21.5	21.7	22.0	22.3	22.8														
0.60	-5.0	-3.6	-2.6	-1.0	0.2	1.3	2.5	3.7	4.9	6.2	7.5													
	22.3	22.3	22.5	22.7	22.9	23.1	23.4	23.8	24.1	24.6														
0.56	-5.4	-3.7	-2.6	-1.0	0.4	1.6	2.8	4.0	5.3	6.6														
	24.0	24.1	24.3	24.6	24.9	25.1	25.4	25.8	26.1															
0.52	-5.5	-3.6	-2.0	-0.6	0.7	2.0	3.2	4.4																
	26.1	26.3	26.6	26.9	27.1	27.4	27.6																	
0.48	-5.3	-3.3	-1.7	-0.2	1.1	2.3	3.6																	
	28.4	28.8	29.1	29.3	29.5	29.7																		
0.44	-4.7	-2.9	-1.3	0.1	1.4	2.5																		
	30.7	31.2	31.5	31.7	31.8																			
0.40	-3.8	-2.2	-0.8	0.5	1.7																			
	32.8	33.3	33.5	33.6	33.6																			
0.36	-2.7	-1.5	-0.3	0.8																				
	34.2	34.7	34.9	34.9																				
0.32	-1.5	-0.8	0.1																					
	35.0	35.4	35.6																					
0.28	-0.5	-0.2																						
	35.2	35.5																						
0.24																								
0.20																								
0.16																								
0.12																								
0.08																								
0.04																								
0.0																								

ZCENT= 0.0 0.04 0.08 0.12 0.16 0.20 0.24 0.28 0.32 0.36 0.40 0.44 0.48 0.52 0.56 0.60 0.64 0.68 0.72 0.76 0.80 0.84 0.88 0.92

EACH BLOCK IS RADIAL DISPLACEMENT IN MICROINCHES
Z DISPLACEMENT IN MICROINCHES

T=0.6524E-05PROGRAM SPALL COMPLETE FOR SPECIFIED TIME OF PROPAGATION